Ph.D. Dissertation

Low-power Wireless Sensor Networking in Interference Environments

간섭 환경에서 저전력 무선 센서 네트워킹에 관한 연구

Jin-Seok Han

February 2017

School of Electrical Engineering and Computer Science
College of Engineering
Seoul National University

Low-power Wireless Sensor Networking in Interference Environments

By

Jin-Seok Han

Submitted to the School of Electrical Engineering and Computer Science
in partial fulfillment of the requirements for the degree of
Ph.D. in Electrical Engineering and Computer Science

at

Seoul National University

February 2017

Committee in Charge:

Professor	Saewoong Bahk, Chairman
Professor	Yong-Hwan Lee, Vice-Chairman
Professor	James Won-Ki Hong
Professor	Daesik Hong
Professor	Sunghyun Choi

Abstract

The demand for commercial deployment of large-scale wireless sensor networks (WSNs) has rapidly been increasing over the past decade. However, conventional WSN technologies may not be feasible for commercial deployment of large-scale WSNs because of their technical flaws, including limited network scalability, susceptibility to co-channel interference and large signaling overhead. In practice, low-power WSNs seriously suffer from interference generated by coexisting radio systems such as IEEE 802.11 wireless local area networks (WLANs). This interference problem seriously hampers commercial deployment of low-power WSNs. Few commercial WSN chips can provide secure and reliable networking performance in practical operation environments.

In this dissertation, we consider performance improvement of low-power WSNs in the presence of co-channel interference. We first investigate the effect of co-channel interference on the transmission of low-power WSN signal, and then design a low-power WSN transceiver that can provide stable performance even in the presence of severe co-channel interference, while providing the backward compatibility with IEEE 802.15.4.

We also consider the network connectivity in the presence of co-channel interference. The connectivity of low-power WSNs can be improved by transmitting synchronization signal and making channel hand-off in a channel-aware manner. A beacon signal for the network synchronization is repeatedly transmitted in consideration of channel condition and signaling overhead. Moreover, when the channel is severely interfered, all devices in

a cluster network make communications by means of temporary channel hopping and then seamlessly make channel hand-off to the best one among the temporary hopping channels. The performance improvement is verified by computer simulation and experiment using IEEE 802.15.4 motes in real operation environments.

Finally, we consider the signal transmission in the presence of co-channel interference. The throughput performance of low-power WSN transceivers can be improved by adjusting the transmission rate and the payload size according to the interference condition. We estimate the probability of transmission failure and the data throughput, and then determine the payload size to maximize the throughput performance. It is shown that the transmission time maximizing the normalized throughput is little affected by the transmission rate, but rather by the interference condition. The transmission rate and the transmission time can independently be adjusted in response to the change of channel and interference condition, respectively. The performance improvement is verified by computer simulation.

Keywords: Low-power wireless sensor network, co-channel interference, interference-robust networking, low-power transceiver, ZigBee.

Student number: 2012-30237

Contents

List of Figures

List of Tables

Chapter 1

Introduction

Recent advances in semiconductor, sensors/actuators and communication technologies have made commercial deployment of a new IT world, referred to Internet-of-Things (IoT), quite feasible. IoT can make connection of enormous number of “things” which can produce and process data in physical and cyber world. Wireless sensor networks (WSNs) play a key role for IoT services by providing real-time connection of the physical world. Since it is required to provide secure connection of a large number of things for IoT services, the industry has been looking for technologies for the large-scale connectivity. For example, electronic shelf label (ESL) services in a mart may need wireless connectivity of at least several thousand of price tags [1]. For commercial deployment of IoT services, it may be required to use WSN technologies that can support the following requirements.

- **Connectivity**: WSN should be able to make secure connection of a large number of nodes as a single network. In practice, however, most of conventional WSN technologies (e.g., ZigBee, Z-Wave and Bluetooth low energy (BLE)) cannot support the construction of a large-scale WSN. It is mainly because they need to operate in

power-, complexity- and capacity-limited environments in addition to limited networking protocol capability. Moreover, the node connectivity may seriously suffer from interference from coexisting radio systems (e.g., wireless local area networks (WLANs) in 2.4 GHz industrial, scientific and medical (ISM) band). WSN should be able to have high networking scalability and fast self-healing capability without large signaling overhead.

- **Reliability**: WSNs should be able to handle data traffic with desired quality of service (QoS) while providing security. However, large-scale WSNs operating in unlicensed spectrum bands may seriously suffer from low traffic reliability mainly due to the presence of interference from coexisting radio systems, hidden node collision and random access collision. They may also suffer from traffic bottleneck at the vicinity of a sink node due to limited transmission capacity. They need to employ a medium access control (MAC) and networking protocol that can provide desired QoS even in harsh operation environments.
- **Power consumption**: Most of WSN nodes are battery-powered, yielding a critical concern on the power consumption for network operation. The power consumption can be saved by making the network operation with low processing complexity and low signaling overhead in addition to low duty-cycle operation. Nevertheless, WSNs seriously suffer from high power consumption due to malfunctioning in the presence of co-channel interference and traffic collision.
- **Cost**: WSNs should be installed and operate at low cost for commercial IoT services. All the MAC and networking mechanisms including node addressing, multi-hop routing, and interference management should work in a simple manner for low-cost implementation. Moreover, WSNs should be able to make connection to a global network at a minimal communication and implementation cost.

IEEE 802.15.4 is a standardized specification applicable to the construction of low-power large-scale WSNs operating in the 2.4 GHz ISM and 900 MHz unlicensed spectrum band [2]. Its MAC protocol supports two operating modes; non-beacon-enabled mode and beacon-enabled mode. In a non-beacon-enabled star topology network, the network coordinator should always be awake for network operation. Devices associated to a network send data to the coordinator or request data from it by using carrier sense multiple access with collision avoidance (CSMA/CA). In a non-beacon-enabled peer-to-peer topology network, devices associated to a network have to keep their radio on constantly or employ a synchronization mechanism to make communications. However, such a mechanism has not yet been supported by the standardization. On the other hand, the beacon-enabled mode can be employed to facilitate low-power operation with the use of a periodic super-frame structure. The super-frame comprises a beacon frame, an active and an inactive period. The network coordinator periodically transmits a beacon frame for synchronous operation with the associated devices at the beginning of the super-frame. Thus, devices in a network as well as the coordinator can periodically switch to a low-power sleep mode, making it possible to operate the network with low-power consumption [3-5]. The active period comprises the contention access period (CAP) and the contention-free period (CFP), making it possible to support traffic requiring low latency or specific data bandwidth.

With IEEE 802.15.4, ZigBee can be applied to the construction of a cluster-tree structured large-scale WSN [6]. It can support low-complexity routing with the use of a distributed address assignment mechanism (DAAM). In practice, however, ZigBee cannot securely construct a large-scale WSN due to some critical flaws, including

networking failure and beacon collision problems [7]. It may also seriously suffer from co-channel interference and network impairments [8, 9], frequently disrupting the network operation. Moreover, when a router node is disassociated from the network, all its child nodes have to individually re-associate to the network, which may require large message exchanges and energy consumption as well. ZigBee may not reliably handle traffic even in the absence of interference as the network size increases. This is mainly because ZigBee employs a CSMA/CA mechanism which is quite subject to hidden node collision [2]. Thus, ZigBee has not successfully been applied to commercial WSN markets.

A number of works considered the coexistence of heterogeneous radio systems operating in unlicensed spectrum bands. It is well recognized that IEEE 802.11x WLAN is one of major interference sources that seriously hamper the operation of low-power WSNs [10-15]. A simple technique is to allocate transmission resource of WSN and WLAN devices orthogonal to each other or to exploit the utilization of white space [16-19]. Channel hopping mechanisms can be employed for low-power WSNs to alleviate the interference problem [20, 21]. For example, IEEE 802.15.4e employs a deterministic synchronous multi-channel extension (DSME) mechanism that can provide channel diversity through channel hopping and channel adaptation [22]. BLE employs an adaptive frequency hopping (AFH) mechanism [23]. However, these approaches may not be effective as the amount of interference sources increases [24-26]. Although WLAN devices employ a channel sensing scheme, they may not detect the presence of low-power WSN signals [27]. In practice, they may transmit signal indifferently from the presence of low-power WSN signals, seriously hampering the transmission of low-power WSN signal.

Some works also considered the employment of a special device so that low-power WSNs can share transmission channel with WLANs. A special device, referred to signaler, may help other ZigBee devices to access channel by sending busy tone, enforcing WLAN devices to defer their transmissions [27]. However, the coordination among the signaler and other ZigBee devices may not be simple, making it inapplicable to practical operation environments. Another special device, referred to arbitrator, can schedule the activity of ZigBee and WLAN devices [28]. However, it may not be easy for the scheduling in dynamic interference environments since it needs to re-initiate spectrum scanning and re-allocate the parameters for the scheduling.

Previous works also considered performance improvement of low-power WSNs in the presence of co-channel interference by means of two approaches; collision-recovery and collision-avoidance approach. The collision-recovery approach aims to mitigate the co-channel interference by using a forward error correction (FEC) technique. For example, BuzzBuzz employs a Hamming(12,8) code-based FEC scheme for ZigBee devices [29]. However, it may not be effective in dynamic interference environments. A real-time adaptive transmission (RAT) scheme makes WSN devices choose an FEC coding scheme to maximize the throughput [30]. However, these collision recovery schemes may not be effective unless the signal-to-interference-plus-noise ratio (SINR) is sufficiently high. Fig. 1-1 illustrates the SINR of IEEE 802.15.4 in the presence of co-channel interference. For example, IEEE 802.15.4 requires an SINR of higher than 0.4 dB for the transmission of 20-byte packets (refer to Chapter 2.2). However, the SINR may not be high enough in practical operating environments, making the collision-recovery approach ineffective for reliable signal transmission.

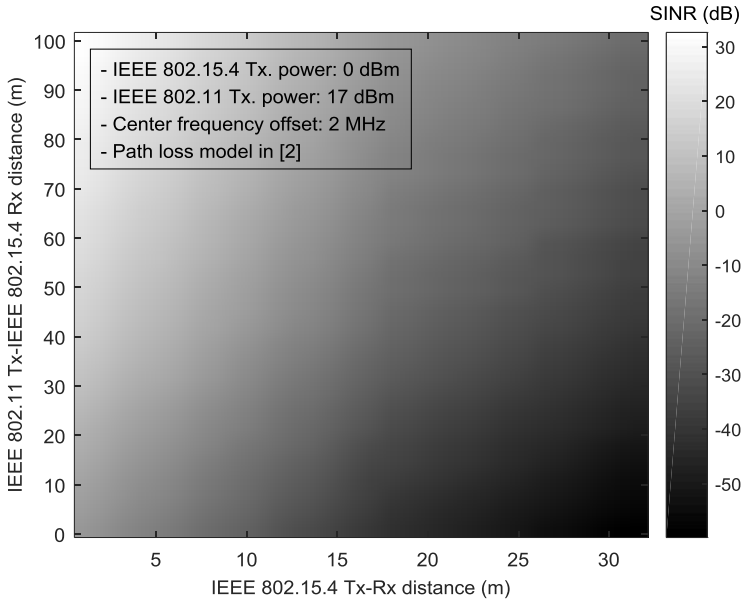

Fig. 1-1. SINR of IEEE 802.15.4 in the presence of co-channel interference.

The collision-avoidance approach aims to escape from co-channel interference by exploiting white space. A dynamic rate adaptation and control for energy reduction (DRACER) scheme adjusts the transmission rate according to the change of operating condition [31]. DRACER may reduce the probability of collision with interference signal by transmitting packets at the highest rate. However, it does not consider the effect of the packet size, yielding inefficient use of white space in the presence of interference. A white space-aware frame adaptation (WISE) scheme considers the adjustment of packet size [24]. Modeling the idle period of interference as a Pareto-distributed random variable, WISE adjusts the packet size to maximize the throughput efficiency, while providing desired packet collision probability. However, it may need to periodically adjust the Pareto model through channel sensing, which may be a considerable processing overhead to low-power WSN devices. Another scheme, referred to dynamic packet length control

(DPLC), simply adjusts the packet size based on a transmission efficiency metric after a number of packet transmissions [32]. However, DPLC may not properly work in the presence of time-varying interference. These collision-avoidance schemes consider the signal transmission at a fixed rate, which may not be efficient when the signal-to-noise power ratio (SNR) is higher than that required for the fixed rate. A scheme that can adjust the payload size and transmission rate of WLANs was proposed in slow fading channel environments [33]. However, it does not consider the presence of co-channel interference, making it impractical for application to low-power WSNs.

As another collision-avoidance approach, partial packet recovery (PPR) techniques can be employed to reduce the transmission of acknowledgement (ACK) packets. They partition a data packet into a number of small blocks and acknowledge the transmission of multiple data packets by transmitting a single recovery frame including a block map that describes the status of all blocks [34-37]. The transmitter should retransmit all the packets when the recovery frame is not received [34] or wait until it receives the recovery frame, and the receiver retransmits the recovery frame until it receives data packets [35-37]. Thus, the PPR techniques may severely suffer from frequent loss of recovery frames in practical operation environments. They do not consider the waiting time when they evaluate the throughput and energy consumption. They may consume energy for the idle listening of WLAN and ZigBee devices as much as for the signal reception [38]. Moreover, these schemes only consider the transmission at a fixed rate.

Most of previous works considered the operation of small scale WSNs in a non-beacon mode, making it inapplicable to IEEE 802.15.4 beacon-enabled large-scale WSNs. IEEE 802.15.4 beacon-enabled WSNs require reliable transmission of synchronization

signal, referred to a beacon frame [39]. It is of great concern how reliably beaconing devices (i.e., the coordinator and routers) can deliver beacon frames to their child devices even in the presence of interference. When a child device fails to receive a beacon frame, it should turn on the transceiver until the reception of a beacon frame, which may result in significant power consumption and transmission delay as well. It is also required to maintain reliable transmission performance even in the presence of interference. It may be desirable to maintain the network connectivity in a distributed manner since multi-hop WSNs may suffer from local interference sources [40], making it difficult to use a single clear channel.

A pseudo random channel hand-off (PRCH) scheme was proposed to escape from co-channel interference by means of channel hand-off [41]. Once detecting the presence of interference, PRCH makes devices switch the transmission channel to a new one determined in a pseudo-random manner. It makes the devices share the information on channel hand-off in advance, making it easy to switch the channel in the presence of interference. However, since the hand-off channel is pseudo-randomly determined without consideration of operating environments, it may still be subject to interference when plural and/or wide bandwidth interference signals exist. IEEE 802.15.4e employs a deferred beacon method (DBM) to alleviate the transmission problem due to the co-channel interference [42]. DBM can improve the transmission reliability by making the coordinator perform channel sensing before the transmission of a beacon frame. However, it may not provide desired performance in the presence of severe interference. Moreover, it may not work properly in hidden node environments since only the transmitter

performs the channel sensing. It may be desirable to employ a scheme properly working in the hidden node environments as well.

In this dissertation, we consider the operation of low-power WSNs in the presence of co-channel interference. We first investigate the effect of co-channel interference on the signal transmission in low-power WSNs. Then, we design a low-power WSN transceiver stably operating in the presence of co-channel interference signal, while providing the backward compatibility with IEEE 802.15.4.

We consider the network connectivity in the presence of co-channel interference. We may improve the connectivity of low-power WSNs by transmitting synchronization signal and making channel hand-off in a channel-aware manner. When a beacon frame is not successfully transmitted, a cluster head and its child devices estimate the channel condition. According to the estimated channel condition, the beacon frame is repeatedly transmitted for reliable delivery. The devices in the cluster can seamlessly make channel hand-off after temporary frequency hopping in the presence of severe interference. They determine the hand-off channel by the best one among the frequency hopping channels which can be pre-determined in consideration of the characteristics of major interference source. We analytically evaluate the performance of the proposed scheme by modeling the presence of major interference signal as a semi-Markov process [43, 44]. We also experimentally evaluate the performance of the proposed scheme using IEEE 802.15.4 TelosB motes in real operation environments [45].

We also consider the signal transmission in the presence of co-channel interference. We may improve the throughput performance of low-power WSNs by adjusting the transmission rate and the payload size according to the interference condition. We assume

that low-power WSNs can support bulk transfer of large data (e.g., e-Price tags [1], surveillance applications involving imaging/acoustics [46, 47], structural health monitoring [48, 49]). Estimating the probability of transmission failure and the data throughput, we determine the payload size to maximize the data throughput in the presence of interference. It is shown that the transmission time maximizing the normalized throughput is little affected by the transmission rate, rather mostly by the interference condition. We independently adjust the payload size and the transmission rate to maximize the data throughput in response to the change of operation environments. Finally, we evaluate the performance of the proposed scheme by computer simulation.

Following Introduction, Chapter 2 describes the system model in consideration and analyzes the effect of co-channel interference on the transmission of IEEE 802.15.4 signal. Chapter 3 and 4 describe how the network connectivity and the transmission performance can be improved in the presence of co-channel interference, respectively. Finally, Chapter 5 summarizes conclusions and issues for further works.

Chapter 2

Effect of co-channel interference on the IEEE 802.15.4 networks

In this chapter, we describe the system model in consideration and analyze the effect of co-channel interference on the transmission of IEEE 802.15.4 signal.

2.1. ZigBee/IEEE 802.15.4-based cluster-tree networks

As illustrated in Fig. 2-1, we consider a ZigBee/IEEE 802.15.4-based cluster-tree structured WSN comprising a network coordinator, depicted by a star symbol, routers, depicted by rectangular symbols, and end devices [6]. The coordinator has no parent node and other nodes can have only one parent node. The coordinator and a router can form a cluster comprising its child routers and end devices as a cluster head. A ZigBee network can utilize one of 16 non-overlapped channels in the 2.4 GHz unlicensed ISM band [6].

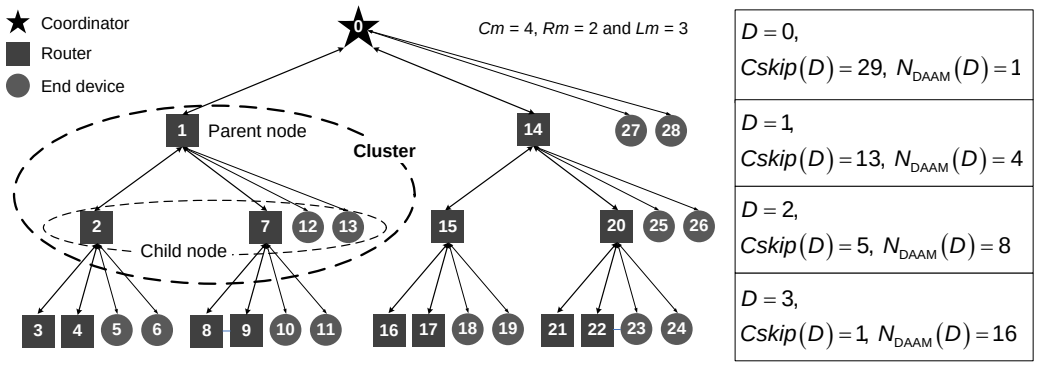

Fig. 2-1. An example of ZigBee DAAM addressing tree.

Fig. 2-2 illustrates an example of IEEE 802.15.4 super-frame structure. Each cluster operates using its own periodic super-frame structure for synchronized network operation [6]. Cluster head r makes synchronization with its child nodes by transmitting beacon frames at an interval of T_{BI}. After transmitting a beacon frame, it can communicate with its child nodes during its active period $T_{SD,r}$. The cluster head and its child nodes can enter a power-saving idle mode during the inactive period. During the active period, the cluster head turns on the receiver for communications with its child nodes. The active period comprises contention access period (CAP) and contention free period (CFP). During the CAP, nodes contend for medium access using a slotted CSMA/CA mechanism. The CFP can be used to support guaranteed medium access and be divided into a number of guaranteed time slots (GTSs). Each child nodes activates its receiver before the beginning of the active period and searches for a beacon frame transmitted from its parent node. If it does not receive a beacon frame, it repeats the beacon reception process maximally N_{sync} times. If it does not receive a beacon frame N_{sync} times consecutively, it becomes an orphan node and needs to initiate the network rejoining process. When a

router becomes an orphan node, its child nodes also become orphan nodes and have to initiate the network rejoining process.

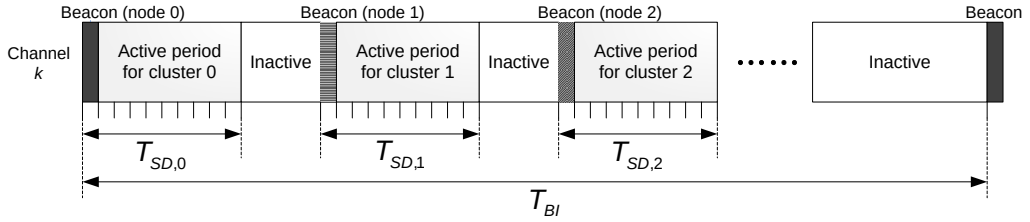

Fig. 2-2. An example of IEEE 802.15.4 super-frame structure.

DAAM can construct a hierarchical addressing tree structure using three addressing parameters; the maximum number of child nodes, *Cm*, the maximum number of child routers, *Rm*, and the maximum network depth, *Lm*. Each router with a network depth smaller than *Lm* uniquely has its own *Cm*-address space to allocate the address to its child nodes (i.e., *Rm* addresses for child routers and (*Cm*-*Rm*) addresses for child end devices). DAAM can effectively make data routing by providing a routing path based on the address information. When a router receives a packet, it can identify whether the destination node of the packet belongs to its sub-tree or not. If the destination node belongs to its descendant node, the router relays the packet to its child node whose sub-tree includes the destination node. Otherwise, it sends the packet to its parent node.

The network coordinator begins network construction with a network depth of zero, while the other nodes try to join the network as an orphan node. For the network joining, a node n first receives beacon frames transmitted from adjacent nodes and initializes a set of potential parent nodes, $\mathbf{P}_n$. It selects a node P_n with the minimum network depth in $\mathbf{P}_n$ as its potential parent node and then requests node P_n for the network joining.

Node P_n accepts the joining request in a first-come and first-served (FCFS) manner when it has an address space available for the requested node type. Each node first requests the network joining as a router. After failing to join the network as a router, it retries to join the network as an end device. After receiving the joining response message, node *n* becomes a child node of P_n with a network depth larger than that of P_n by one. When the joining request is denied, node n deletes P_n from $\mathbf{P}_n$ and repeats the network joining process by selecting another potential parent node in $\mathbf{P}_n$ until $\mathbf{P}_n = \varnothing$. If a node joins the network as a router, it periodically transmits beacon frames, allowing neighboring nodes to detect its presence. However, ZigBee does not suggest a specific beacon scheduling method.

2.2. Performance of IEEE 802.15.4 transceiver

We analyze the packet error rate (PER) of IEEE 802.15.4 in the presence of additive channel noise and wideband interference signals. IEEE 802.15.4 employs a quasi-orthogonal modulation scheme, where each symbol is represented by one of 16 pseudo-random sequences. It can achieve a direct sequence spread spectrum-like processing gain, which is effective to the presence of interference signal whose bandwidth is smaller than that of IEEE 802.15.4 signal (e.g., Bluetooth signal with 1MHz bandwidth).

However, when wideband interference signal such as WLAN signal exists, it may behave to the IEEE 802.15.4 signal like white additive noise. Thus, the receiver performance of IEEE 802.15.4 in the presence of WLAN signal can be approximated by

that in additive white Gaussian noise (AWGN) channel. The bit error rate (BER) of IEEE 802.15.4 PHY can be represented as [2]

$$b(\gamma) = \frac{8}{15} \times \frac{1}{16} \times \sum_{k=2}^{16} (-1)^k \binom{16}{k} e^{20\gamma\left(\frac{1}{k}-1\right)} \tag{2.1}$$

where γ_I denotes the SINR given by

$$\begin{aligned} \gamma_I &= \frac{P_{\mathrm{r}}}{\sum_i P_{\mathrm{Int},i} + P_{\mathrm{n}}} \\ &= \frac{10^{PL(d)/10} P_{\mathrm{t}}}{\sum_i \left(10^{PL(d_{\mathrm{Int},i})/10} \int_{BW_{\mathrm{r}}} S_{\mathrm{Int},i}\, df \right) + P_{\mathrm{n}}} \end{aligned} \tag{2.2}$$

where P_{r}, P_{Int} and P_{n}, respectively, denotes the received signal power, interference signal power, and noise power, BW_{r} denotes the signal bandwidth, S_{Int} denotes the power spectral density of interference signal, and $PL(d)$ is the path-loss in dB, given by [2]

$$PL(d) = \begin{cases} 40.2 + 20\log_{10} d + NF, & d \le 8 \ (m) \\ 58.5 + 33\log_{10}(d/8) + NF, & d > 8 \ (m). \end{cases} \tag{2.3}$$

Here NF denotes the noise figure and d is the distance between the transmitter and receiver. In the presence of WLAN interference signal, the SINR can be approximated as

$$\gamma_I \approx \frac{10^{PL(d)/10} P_{\mathrm{t}}}{\sum_i \left(10^{PL(d_{\mathrm{Int},i})/10} \frac{BW_{\mathrm{r}}}{BW_{\mathrm{WLAN,i}}} P_{\mathrm{Int},i} \right) + P_{\mathrm{n}}} \tag{2.4}$$

where BW_{WLAN} denotes the WLAN signal bandwidth. Note that only a fraction of the WLAN signal power affects the IEEE 802.15.4 reception. However, IEEE 802.15.4

WPAN is still susceptible to the presence of WLANs which have transmit power higher than IEEE 802.15.4 by 20 dB. Then, it can be shown that the PER of IEEE 802.15.4 in the presence of AWGN and multiple WLANs, say p, is represented as

$$p = 1 - \left(1 - b(\gamma)\right)^{L} \tag{2.5}$$

where L denotes the packet size.

The minimum SINR to achieve a desired PER of p_s with the use of packet size L can be represented as

$$\hat{\gamma} = b^{-1}\left(1 - p_s^{1L/}\right) \tag{2.6}$$

where b denotes the BER and b^{-1} denotes its inverse. Since the BER is a decreasing function of SINR, it can be seen that $b(\gamma)$ has an inverse function. However, it may not be feasible to obtain the inverse function of (2.1) in a closed-form. A numerical method can be applied to approximately calculate (2.6). Table 2-1 summarizes the minimum SINR according to the packet size L.

Table 2-1. Minimum SINRs for IEEE 802.15.4 communications.

L	20 bytes	40 bytes	60 bytes	80 bytes	100 bytes	120 bytes
$\hat{\gamma}$	0.40 dB	0.68 dB	0.83 dB	0.93 dB	1.01 dB	1.07 dB

Chapter 3

Performance improvement of network connectivity in interference environments

In this section, we consider performance improvement of a beacon-enabled cluster-tree WSNs by means of channel-aware signal transmission and channel hand-off in the presence of co-channel interference. When the beacon transmission is failed, the cluster head and its child devices estimate the channel condition. According to the estimated channel condition, the cluster head repeatedly transmits the beacon frame for reliable delivery. The proposed scheme makes the devices seamlessly hand-off the channel through temporary frequency hopping in the presence of severe interference. The final hand-off channel is determined by the best one among the frequency hopping channels. Representing the presence of major interference signal as a semi-Markov process [43, 44], we analytically evaluate the performance of the proposed scheme. We also experimentally evaluate the performance of the proposed scheme using IEEE 802.15.4 TelosB motes in real operation environments [45].

3.1. System model

As illustrated in Fig. 3-1, we consider an IEEE 802.15.4-based beacon-enabled cluster-tree WSN comprising a network coordinator, routers and end devices located in the presence of WLANs. The IEEE 802.15.4 network can utilize one of 16 non-overlapped channels in the 2.4 GHz ISM band, whose center frequency is determined by

$$f(k_c) = 2405 + 5(k_c - 11), \quad k_c = 11, 12, \ldots, 26 \tag{3.1}$$

where k_c denotes the channel index. We assume that all the devices in the network use the same channel k determined in the initialization process.

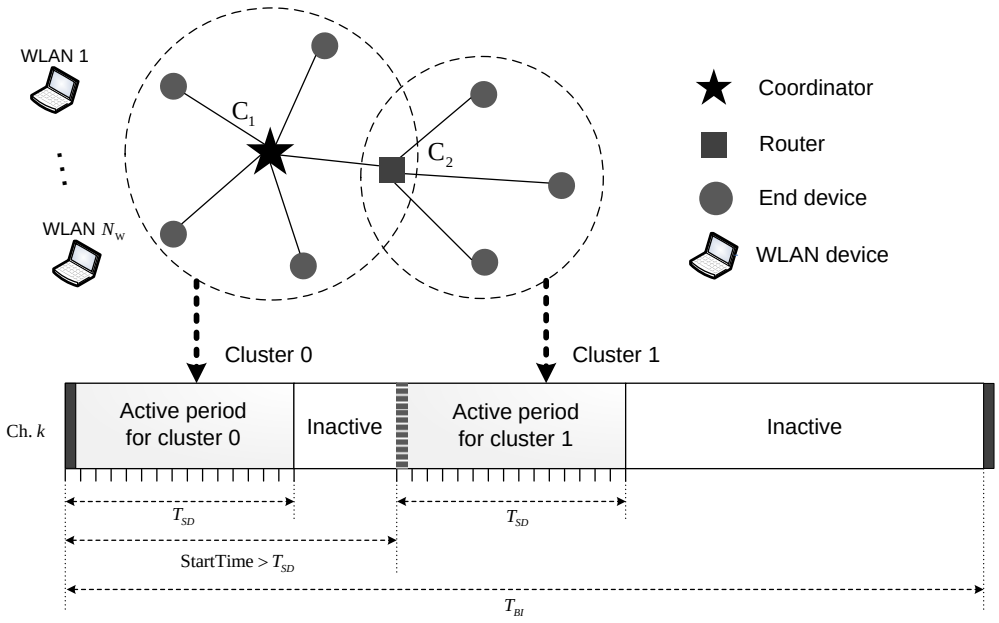

Fig. 3-1. Operation of an IEEE 802.15.4-based beacon-enabled cluster-tree WSN.

A beacon-enabled cluster-tree WSN can have multiple clusters, each of which comprises a cluster head and its child devices. We assume that each cluster operates using its own periodic super-frame structure as illustrated in Fig. 3-1. At the beginning of the active period, the cluster head transmits a beacon frame for synchronized transaction with its child devices. The beacon interval and the super-frame duration are determined as, respectively,

$$T_{BI} = \left(aBaseSuperframeDuration \cdot 2^{BO} \right) t_{sym}, \quad \text{for } 0 \le BO \le 14 \tag{3.2}$$

$$T_{SD} = \left(aBaseSuperframeDuration \cdot 2^{SO} \right) t_{sym}, \quad \text{for } 0 \le SO \le BO \tag{3.3}$$

where BO is the beacon order, SO is the super-frame order and t_{sym} is the symbol time. The child devices in each cluster can make communications with their parent device only during the active period, while entering a power-saving idle mode during the inactive period. The child device activates its receiver before the beginning of the super-frame and searches for a beacon frame transmitted from its parent device. If it does not receive a beacon frame within a time interval of T_{sync} seconds, it repeats the beacon reception process maximally N_{sync} times. If it does not receive a beacon frame consecutively N_{sync} times, it becomes an orphan node and may need to initiate the network rejoining process.

Losses of beacon frame can occur mainly due to the collision with signal generated by other radio systems or channel errors. A channel error can occur when the SINR is lower than a certain threshold. The failure probability of beacon reception on channel k can be represented as

$$\tilde{p}_k = 1 - \left(1 - p_k\right)\left(1 - p_k^e\right) \tag{3.4}$$

where p_k and p_k^e denote the failure probability of beacon reception on channel *k* due to the collision and the channel error, respectively. The probability of channel error can be calculated by $p_k^e = 1 - \left(1 - b_k^e\right)^n$, where n denotes the bit size of the beacon frame and b_k^e denotes the BER of IEEE 802.15.4 signal on channel *k*. Note that there may be interference from various sources such as a nearby IEEE 802.15.4 network operating on adjacent channels [50]. However, the proposed scheme works without identifying the resource of interference.

The failure probability of beacon reception due to the collision can be calculated from the channel occupancy model of interference signal. We characterize the presence of interference using a simple semi-Markov model obtained from the analysis of WLAN channel usage pattern in [43, 44], which is the major interference source in the 2.4 GHz ISM band[1]. The channel has two operation states, busy and idle state, whose duration is described by probability density function $f_{T_{busy,k}}(t)$ and $f_{T_{\text{idle},k}}(t)$, respectively. Then, the interference occupancy ratio of channel k can be defined by

$$\rho_k = \frac{\tau_{\text{busy},k}}{\tau_{\text{busy},k} + \tau_{\text{idle},k}} \tag{3.5}$$

where $\tau_{\text{busy},k}$ and $\tau_{\text{idle},k}$ denote the mean duration of busy and idle state on channel k, respectively. It can be shown that p_k can be represented as

[1] The semi-Markovian assumption is that the duration of idle states is independent of each other. It was shown from extensive measurement in [44] that the assumption can be valid when the temporal separation is large (e.g., WSNs operating with a long duty cycle).

$$p_k = \rho_k p_{k|\text{busy}} + (1-\rho_k)\, p_{k|\text{idle}} \tag{3.6}$$

where $p_{k|\text{busy}}$ and $p_{k|\text{idle}}$ denote the failure probability of beacon reception due to the collision in the presence and the absence of interference signal on channel k, respectively. Define the average synchronization time T_k on channel k by the average time interval between two successful beacon receptions. Then, it can be shown that

$$\begin{aligned} T_k &= (1-\tilde{p}_k) T_{BI} + \tilde{p}_k (1-\tilde{p}_k) 2T_{BI} + \tilde{p}_k^2 (1-\tilde{p}_k) 3T_{BI} + \cdots \\ &= \frac{1}{1-\tilde{p}_k} T_{BI}. \end{aligned} \tag{3.7}$$

3.2. Previous works

We briefly review beaconing and channel hand-off schemes proposed for IEEE 802.15.4-based WSNs, and analyze their performance in terms of the failure probability of beacon reception and the average synchronization time. Hereafter p_k is referred to the failure probability of beacon reception.

3.2.1. IEEE 802.15.4 periodic beacon method (PBM)

The cluster head periodically transmits a beacon frame without consideration of channel condition. If the beacon frame is transmitted during the interference busy state, it may collide with interference signal with probability $p_{\text{PBM},k|\text{busy}} = 1$. When the beacon frame is transmitted during the interference idle state, it may probabilistically experience packet collision. When an interference source transmits signal after energy-based clear channel assessment (CCA), it may not detect IEEE 802.15.4 beacon frames unless it is located near the beacon transmitter. When an interference source transmits signal after

carrier sensing-based CCA, it may not detect IEEE 802.15.4 beacon frames and cause the collision. It can be shown that the failure probability of beacon reception can be represented as

$$p_{\mathrm{PBM},k} = \begin{cases} \rho_k & ; \text{ when interference source on a frame} \\ \rho_k + (1-\rho_k)\, p_{\mathrm{PBM},k|\mathrm{idle}} & ; \text{ otherwise} \end{cases} \tag{3.8}$$

where $p_{\mathrm{PBM},k|\mathrm{idle}}$ is the probability $p_{k|\mathrm{idle}}$ of PBM and can be derived as follows. For given idle state length T_{idle} and beacon frame length T_b, a packet collision may occur if the beacon frame is transmitted $(T_{\mathrm{idle}} - T_b)$ seconds later than the beginning of the idle state. Let Δ be the time difference between when an idle state starts and when a beacon frame is ready for transmission (i.e., $0 \le \Delta \le T_{\mathrm{idle}}$). Assuming that the duration of the idle state is Pareto or exponentially distributed [43, 44], it can be shown that

$$\begin{aligned} p_{\mathrm{PBM},k|\mathrm{idle}}(\Delta) &= \Pr[T_{\mathrm{idle}} < \Delta + T_b \mid \Delta] \\ &= \begin{cases} 1 - \left(\dfrac{\Delta}{\Delta + T_b}\right)^{\beta_k} & ; \text{ Pareto d} \\ 1 - e^{-\tau_{\mathrm{idle}}^{-1} T_b} & ; \text{ exp} \end{cases} \end{aligned} \tag{3.9}$$

where β_k denote the shape parameter of Pareto distribution of channel *k*. It can be seen that the probability depends on Δ when the idle state is Pareto distributed. On the other hand, it can also be seen that the probability does not depend on Δ when the idle state is exponentially distributed. In this case, the expected failure probability of beacon reception can be represented as

$$p_{\mathrm{PBM},k} = \begin{cases} \rho_k & ; \text{ when interference source on a frame} \\ 1 - (1-\rho_k) e^{-\tau_{\mathrm{idle}}^{-1} T_b} & . \quad ; \text{ other} \end{cases} \tag{3.10}$$

The average synchronization time can be calculated by (3.7).

3.2.2. IEEE 802.15.4e deferred beacon method (DBM)

The cluster head transmits a beacon frame after confirming channel clearance through CCA. When an energy-type detector is employed for the CCA, it can make a decision using a simple hypothesis testing as

$$D_k = \begin{cases} \mathcal{H}_1; & \text{if } y_k = \frac{1}{N}\sum_{j=n-N+1}^{n} |r_k(j)|^2 \geq \eta \\ \mathcal{H}_0; & \text{otherwise} \end{cases} \tag{3.11}$$

where $\mathcal{H}_0$ and $\mathcal{H}_1$ denote simple hypotheses corresponding to the absence and the presence of interference signal on channel k, respectively, r_k denotes the signal received through channel k, y_k is the test statistic, N is the number of samples for the test, and η is a threshold to be determined. When the detection threshold is determined based on the constant false-alarm rate criterion [51], it can be shown for a given target false-alarm probability $\tilde{p}_f$ that the detection probability $p_{d,k}$ can approximately be represented as

$$p_{d,k} \cong Q\left[\left(\frac{Q^{-1}(\tilde{p}_f)}{\sqrt{N}} - \gamma_k\right)\sqrt{\frac{N}{2\gamma_k + 1}}\right] \tag{3.12}$$

where γ_k is the received SNR of channel k.

When a cluster head transmits a beacon frame at time t during the interference busy state, the corresponding failure probability of beacon reception can be represented as

$$p_{\mathrm{DBM},k|\mathrm{busy},t}=\begin{cases}\left(1-p_{d,k}^{m-1}\right)+p_{d,k}^{m-1}\alpha_k;\ 0\le t<\tau_{\mathrm{busy},k}-(m-1)T_u \text{ and } m=\left\lceil \tau_{\mathrm{busy},k}/T_u \right\rceil \\ \left(1-p_{d,k}^{j}\right)+p_{d,k}^{j}\alpha_k;\quad \tau_{\mathrm{busy},k}-(j+1)T_u\le t<\tau_{\mathrm{busy},k}-jT_u \text{ and } j=0,1,\ldots m-2\end{cases} \tag{3.13}$$

where $0\le t<\tau_{\mathrm{busy},k}$, T_u is the channel sensing period and α_k is the failure probability of beacon reception when the cluster head defers the beacon transmission to the beginning of the idle state, represented as

$$\alpha_k=1-\frac{1}{\tau_{\mathrm{idle},k}^{-1}T_u}e^{-\tau_{\mathrm{idle},k}^{-1}(T_u+T_b)}\left(1-e^{-\tau_{\mathrm{idle},k}^{-1}T_u}\right). \tag{3.14}$$

It can easily be shown that the corresponding failure probability of beacon reception can be represented as

$$\begin{aligned}p_{\mathrm{DBM},k|\mathrm{busy}}&=\frac{1}{\tau_{\mathrm{busy},k}}\int_0^{\tau_{\mathrm{busy},k}}p_{\mathrm{DBM},k|\mathrm{busy},t}\,dt\\&=1-(1-\alpha_k)\left\{\frac{T_u}{\tau_{\mathrm{busy},k}}\sum_{j=0}^{m-1}p_{d,k}^{j}+\left(1-\frac{T_u}{\tau_{\mathrm{busy},k}}m\right)p_{d,k}^{m-1}\right\}.\end{aligned} \tag{3.15}$$

When the cluster head transmits a beacon frame during the interference idle state, the corresponding failure probability of beacon reception can be represented as

$$\begin{aligned}p_{\mathrm{DBM},k|\mathrm{idle}}&=\tau_{\mathrm{idle},k}^{-1}\left[\int_0^{T_u+T_b}\left(\int_0^{t-T_s}di+\int_{t-T_s}^{t}1-p_d^{m-1}\,di\right)f_{T_{\mathrm{idle},k}}(t)\,dt\right.\\&\left.\quad+\int_{T_u+T_b}^{\infty}\left(\int_{t-(T_u+T_b)}^{t-T_s}di+\int_{t-T_s}^{t}1-p_d^{m-1}\,di\right)f_{T_{\mathrm{idle},k}}(t)\,dt\right]\\&=1-e^{-\tau_{\mathrm{idle},k}^{-1}(T_u+T_b)}-\tau_{\mathrm{idle},k}^{-1}T_s p_d^{m-1}\end{aligned} \tag{3.16}$$

where T_s is the time for the channel sensing (i.e., the time for each CCA, $T_s<T_u$). When the interference source can detect the beacon frames, $p_{\mathrm{DBM},k|\mathrm{idle}}$ is zero. It can

easily be shown that the expected failure probability of beacon reception can be represented as

$$p_{\mathrm{DBM},k} = \rho_k \left[1-(1-\alpha_k) \left\{ \frac{T_u}{\tau_{\mathrm{busy},k}} \sum_{j=0}^{m-1} p_{d,k}^{j} + \left(1-\frac{T_u}{\tau_{\mathrm{busy},k}} m \right) p_{d,k}^{m-1} \right\} \right] + (1-\rho_k)\left(1-e^{-\tau_{\mathrm{idle},k}^{-1}(T_u+T_b)} - \tau_{\mathrm{idle},k}^{-1} T_s p_{d,k}^{m-1}\right). \tag{3.17}$$

It can be seen that the beacon collision probability is tightly associated with the detection probability p_d.

DBM may not work properly when the interferer is located outside the channel sensing range (i.e., $p_{d,k}=0$). When $p_{d,k}=0$, (3.17) can be rewritten as

$$\begin{aligned} p_{\mathrm{DBM},k} &= \rho_k \left[1-\frac{1}{\tau_{\mathrm{idle},k}^{-1}\tau_{\mathrm{busy},k}} e^{-\tau_{\mathrm{idle},k}^{-1}T_b} e^{-\tau_{\mathrm{idle},k}^{-1}T_u} \left(1-e^{-\tau_{\mathrm{busy},k}^{-1}T_u}\right) \right] \\ &\quad + (1-\rho_k)\left(1-e^{-\tau_{\mathrm{idle},k}^{-1}T_b} e^{-\tau_{\mathrm{idle},k}^{-1}T_u}\right) \\ &\cong \rho_k + (1-\rho_k)\left(1-e^{-\tau_{\mathrm{idle},k}^{-1}T_b}\right) \quad (\because e^{-\tau_{\mathrm{idle},k}^{-1}T_u} \cong 1) \\ &= p_{\mathrm{PBM},k}. \end{aligned} \tag{3.18}$$

It can be seen that DBM provides no performance improvement over PBM. The average synchronization time can be calculated by (3.7).

3.2.3. Pseudo random channel hand-off (PRCH)

PRCH scheme can avoid co-channel interference by means of channel hand-off in a pseudo-random manner. When a cluster head detects the presence of interference by measuring packet errors, it changes the transmission channel to a new channel k_{PR} after transmitting a channel hand-off command to its child devices. It can pseudo-randomly

determine the hand-off channel k_{PR} using a cluster key (e.g., the cluster identifier or cluster head address). Thus, the child devices can make channel hand-off to channel k_{PR} regardless of the reception of a channel hand-off command.

Once a child device receives a channel hand-off command through channel k, it searches for a beacon frame on channel k_{PR} for a maximum interval of T_{sync} seconds. If the child device does not receive a beacon frame on channel k_{PR}, it repeats the beacon search process while increasing the beacon-loss counter $n_{sync,\mathrm{PR}}$ by one. If the counter $n_{sync,\mathrm{PR}}$ reaches a threshold $N_{sync,\mathrm{PR}}$, it becomes an orphan node and may need to initiate the network rejoining process.

If a child device does not receive a channel hand-off command through channel k, its beacon-loss counter $n_{sync,\mathrm{PR}}$ will automatically reach $N_{sync,\mathrm{PR}}$. Then, it makes channel hand-off to channel k_{PR} by itself and searches for a beacon frame for a maximum interval of T_{sync} seconds. If it does not receive a beacon frame within T_{sync} seconds, it repeats the beacon reception process while increasing the beacon-loss counter by one. If $n_{sync,\mathrm{PR}}$ reaches a threshold $N_{sync,\mathrm{PR}}$, the child device becomes an orphan node and may need to initiate the network rejoining process.

Define the interference avoidance time by the time difference between when the cluster head transmits a beacon frame with channel hand-off command and when a child device first receives it on the hand-off channel. Let $T_{IA,\mathrm{PR}}$ be the interference avoidance time with the use of PRCH when the child device receives the channel hand-off command. Then, it can be shown that

$$
\begin{aligned}
T_{IA,\mathrm{PR}} &= \left(1-p_{k_{\mathrm{PR}}}\right)T_{BI} + p_{k_{\mathrm{PR}}}\left(1-p_{k_{\mathrm{PR}}}\right)2T_{BI} + \cdots + p_{k_{\mathrm{PR}}}^{N_{sync,\mathrm{PR}}}\left[\left(N_{sync,\mathrm{PR}}+1\right)T_{BI} + T_{RE}\right] \\
&= T_{BI}\left(1+\sum_{i=1}^{N_{b,\mathrm{PR}}} p_{k_{\mathrm{PR}}}^{i}\right) + T_{RE}\, p_{k_{\mathrm{PR}}}^{N_{sync,\mathrm{PR}}}.
\end{aligned}
\tag{3.19}
$$

Let $T'_{IA,\mathrm{PR}}$ be the interference avoidance time with the use of PRCH when the child device does not receive the channel hand-off command. Then, it can be shown that

$$
\begin{aligned}
T'_{IA,\mathrm{PR}} &= T_{\mathrm{o}} + \left(1-p_{k_{\mathrm{PR}}}\right)T_{BI} + p_{k_{\mathrm{PR}}}\left(1-p_{k_{\mathrm{PR}}}\right)2T_{BI} + \cdots \\
&\quad + p_{k_{\mathrm{PR}}}^{N_{sync,\mathrm{PR}}}\left[\left(N_{sync,\mathrm{PR}}+1\right)T_{BI} + T_{RE}\right] \\
&= T_{\mathrm{o}} + T_{BI}\left(1+\sum_{i=1}^{N_{sync,\mathrm{PR}}} p_{k_{\mathrm{PR}}}^{i}\right) + T_{RE}\, p_{k_{\mathrm{PR}}}^{N_{sync,\mathrm{PR}}}.
\end{aligned}
\tag{3.20}
$$

PRCH may require for an average time of $\bar{T}_{IA,\mathrm{PR}}$ for the interference avoidance, represented as

$$
\begin{aligned}
\bar{T}_{IA,\mathrm{PR}} &= \left(1-p_{k_{\mathrm{PR}}}\right)T_{IA,\mathrm{PR}} + p_{k_{\mathrm{PR}}}\, T'_{IA,\mathrm{PR}} \\
&= \left(T_{\mathrm{o}} - T_{BI}\right)p_{k_{\mathrm{PR}}} + T_{BI}\left(1+\sum_{i=1}^{N_{sync,\mathrm{PR}}} p_{k_{\mathrm{PR}}}^{i}\right) + T_{RE}\, p_{k_{\mathrm{PR}}}^{N_{sync,\mathrm{PR}}}.
\end{aligned}
\tag{3.21}
$$

It can be shown that PRCH takes an average synchronization time represented as

$$
T_{\mathrm{PR}} = \begin{cases} \dfrac{1}{1-p_{\mathrm{PBM},k}}T_{BI} & \text{; before channel hand-off} \\ \dfrac{1}{1-p_{\mathrm{PBM},k_{\mathrm{PR}}}}T_{BI} & \text{; after channel hand-off.} \end{cases}
\tag{3.22}
$$

It can be seen from (3.21) and (3.22) that the interference avoidance time and the average synchronization interval are tightly associated with $p_{k_{\mathrm{PR}}}$. Note that $p_{k_{\mathrm{PR}}}$ depends only on the link quality of channel k_{PR}. Since the hand-off channel k_{PR} is predetermined

without consideration of operation environments, PRCH may suffer from significant performance degradation in the presence of plural and/or wideband interference sources.

3.3. Proposed interference management scheme

We consider the alleviation of co-channel interference problem in IEEE 802.15.4-based WSNs by means of repeated beacon transmission and seamless channel hand-off. Fig. 3-2 illustrates the overall procedure of the proposed scheme.

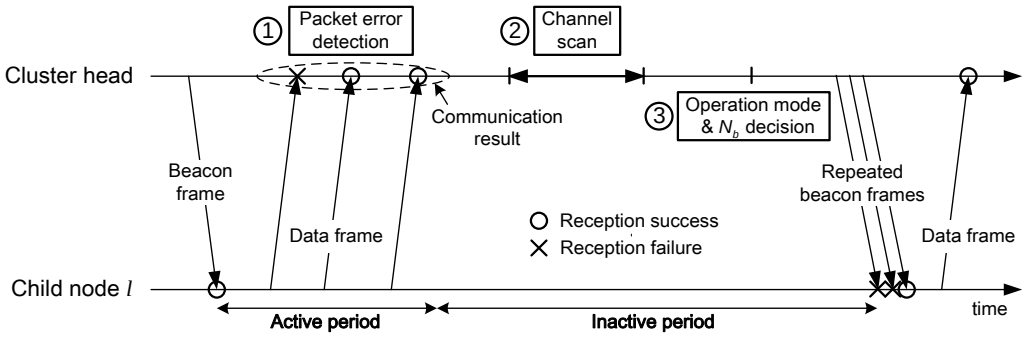

Fig. 3-2. Overall procedure of the proposed scheme.

3.3.1. Interference detection

The presence of interference can be detected by means of packet-error detection and channel scanning in each cluster. Let n_p be the number of packet reception errors of a cluster head during the active period. If n_p reaches a threshold N_p, the cluster head scans channel k during the inactive period excluding the active period of neighboring clusters. In addition, the child device can request the channel scan to its cluster head.

When the PER exceeds a threshold, the child device sends a message indicating the increase of PER to its cluster head, requesting the channel scan.

With the use of an energy-type detector, the cluster head can estimate the channel occupancy ratio as

$$\hat{\rho}_k = \frac{1}{N_{sp}} \sum_{j=1}^{N_{sp}} I\left\{ y_{j,k} \geq \eta \right\} \tag{3.23}$$

where $I\{\cdot\}$ is the indicator function, $y_{j,k}$ is the energy of the j-th sample received on channel k, N_{sp} is the total number of samples for the measurement and η is a threshold to be determined. It can confirm the presence of interference signal on channel k as

$$\varphi_k = \begin{cases} 0\,; & 0 \leq \hat{\rho}_k < \delta_1 \\ 1\,; & \delta_1 \leq \hat{\rho}_k < \delta_2 \\ 2\,; & \hat{\rho}_k \geq \delta_2 \end{cases} \tag{3.24}$$

where δ_1 and δ_2 are thresholds to be determined. If $\varphi_k = 2$, the cluster head confirms the presence of severe interference on channel k, requiring the channel hand-off. If $\varphi_k = 1$, the cluster head confirms the presence of mild interference on channel k. In this case, the cluster head does not initiate the channel hand-off process, but repeatedly transmits the beacon frame according to the estimated channel condition $\hat{\rho}_k$. If $\varphi_k = 0$, the cluster head increases the channel scanning counter n_s by one. If n_s reaches a threshold N_s, the cluster head also confirms the presence of severe interference on channel k. This process can alleviate a hidden node problem (i.e., the case when child devices are interfered, but the cluster head is not). The counter n_s is reset when the channel scan is not required.

3.3.2. Repeated transmission of beacon frame (RTB)

When $\varphi_k = 1$, the cluster head does not initiate the channel hand-off process, but repeatedly transmits the beacon frame according to the estimated channel condition $\hat{\rho}_k$. It determines the number of repeated beacon transmissions, N_b to achieve beacon transmission with desired probability $\tilde{p}_s$ and desired transmission time $T_{SD,\min}$ as

$$\begin{aligned} N_b = & \min_{n_b} n_b \\ & \text{subject to } p_k^{(n_b)} \le 1 - \tilde{p}_s \quad \text{and} \quad (n_b - 1)\left(T_b + \hat{t}_{ibs}\right) > T_{SD} - T_{SD,\min} \end{aligned} \tag{3.25}$$

where $\hat{t}_{ibs}$ denotes the time interval between the transmission of two beacon frames, $p_k^{(n_b)}$ is the probability of n_b beacon collisions on channel k and $T_{SD,\min}$ is the desired minimum transmission time. Making $\hat{t}_{ibs}$ equal to the length of the interference busy state (i.e., $\hat{t}_{ibs} = \hat{\tau}_{\text{busy},k}\left(\tilde{l}\right)$), it can be shown that $p_k^{(n_b)} \cong \left(p_{\text{PBM},k}\right)^{n_b}$. This implies that when the beacon is repeatedly transmitted for a relatively short time interval, the beacon transmissions are statistically independent of each other [9].

It can be shown that the minimum number of beacon transmissions to satisfy the first constraint $p_k^{(n_b)} \le 1 - \tilde{p}_s$ in (3.25) can be determined as

$$N_{b,\min} = \left\lceil \frac{\log\left(1 - \tilde{p}_s\right)}{\log\left[1 - \left(1 - \hat{\rho}_k\right) e^{-\frac{\hat{\rho}_k}{1-\hat{\rho}_k}\frac{T_b}{\tau_{\text{busy}}}}\right]} \right\rceil. \tag{3.26}$$

If $N_{b,\min}$ beacon transmissions can satisfy desired minimum transmission time $T_{SD,\min}$ (i.e., $\left(N_{b,\min} - 1\right)\left(T_b + \hat{t}_{ibs}\right) < T_{SD} - T_{SD,\min}$), the cluster head determines N_b by $N_{b,\min}$. It can be shown that the expected failure probability of beacon reception can be represented as

$$p_{\mathrm{RTB},k}^{(N_b)} = \left\{1-\left(1-\hat{\rho}_k\right)e^{-\hat{\tau}_1^{-1}\,\mathrm{d}\,\mathrm{R}\,T_{\mathrm{b}}}\right\}^{N_b}. \tag{3.27}$$

The average of the corresponding synchronization time can be represented as

$$T_{\mathrm{R\ T\ B}} = \frac{1}{1-\left\{1-\left(1-\hat{\rho}_k\right)e^{-\hat{\tau}_1^{-1}\,\mathrm{d}\,\mathrm{R}\,T_{\mathrm{b}}}\right\}^{N_b}} T_{BI}. \tag{3.28}$$

If the beacon transmission of $N_{b,\min}$ consecutive times cannot provide desired minimum transmission time $T_{SD,\min}$ (i.e., $\hat{\rho}_k \geq \delta_2$), the cluster head confirms that the interference is too severe to maintain the network connectivity through the channel in use and initiates the channel hand-off process to be described in Section 3.3.3. It may be desirable to adjust the number N_b in response to the change of interference and data transmission scheme.

3.3.3. Channel hand-off with the use of channel hopping

When the interference is too severe, it may be desirable to use a new channel to reliably maintain the network operation. When the cluster head detects the presence of severe interference on channel k, it notifies the presence to its child devices by sending a beacon frame containing the channel hand-off command, referred to the hand-off beacon (H-beacon), through channel k. Once the child device receives an H-beacon, it changes the transmission mode, referred to the hand-off mode (H-mode). In the H-mode, the cluster head transmits an H-beacon through a hand-off candidate channel in a frequency hopping manner. The hand-off candidate channels (i.e., frequency hopping channels) can be predetermined in consideration of the characteristics of major interference signal. In practice, the H-beacon may not reliably be delivered to the child devices through channel

k which has already been interfered. This problem can be alleviated by means of the proposed RTB.

Let $\Omega_H = \{k_1, \ldots, k_M\}$ be a set of frequency hopping channels to be used in the H-mode. After detecting the presence of interference signal on channel k, the cluster head repeatedly transmits the H-beacon through channel k at time t_0 and then switches to the H-mode at the next frame time. It transmits an H-beacon at time $t_0 + (Mn + m - 1)T_{BI}$ through channel k_m $(\in \Omega_H)$ determined by a frequency hopping rule, where $1 \le m \le M$ and $n \ge 1$. Fig. 3-3 illustrates an example of the proposed channel hand-off process, where we assume that $k = 11$, $M = 4$ and $\Omega_H = \{15, 19, 23, 11\}$. In the presence of severe interference on channel $k = 11$, the cluster head repeatedly transmits an H-beacon containing a channel hand-off command through channel $k = 11$ and then transmits it through a frequency hopping channel 15, 19, 23 or 11, which is sequentially assigned at the beacon transmission time. After observing the channel condition for a certain number of beacon intervals, the cluster head determines the clearest channel in Ω_H, say channel 15, as the hand-off channel. Finally, all the devices in the cluster use channel 15 for the signal transmission from time when channel 15 is scheduled for the signal transmission (i.e., from time t_{13}), while transmitting a normal beacon frame instead of H-beacon. Note that only clusters that detect the presence of severe interference make the channel hand-off, alleviating the interference problem in a cluster-wise manner.

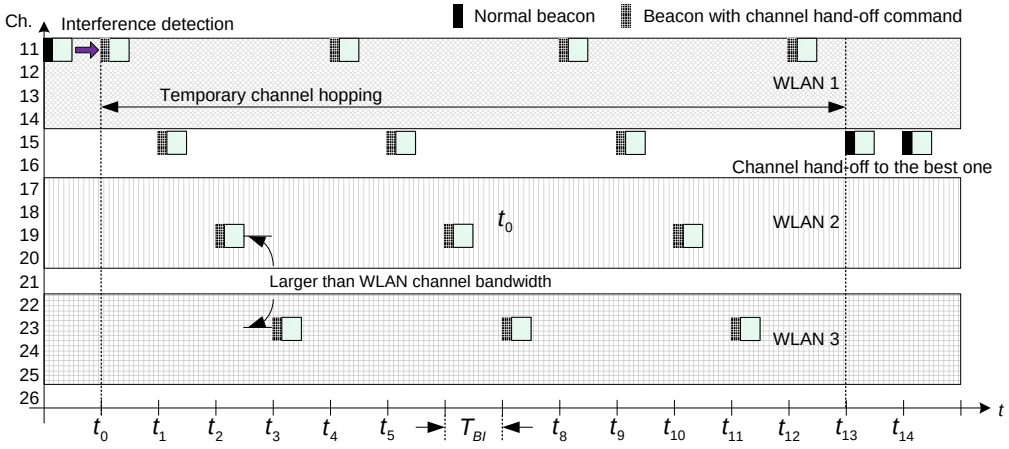

Fig. 3-3. An example of the proposed channel hand-off process when $k = 11$ and $\Omega_H = \{15, 19, 23, 11\}$.

The child devices can make channel hand-off regardless of H-beacon reception on channel k. Once a child device receives an H-beacon on channel k, it searches for an H-beacon on the first candidate channel k_1 in Ω_H for a maximum interval of T_{rx} seconds. If it receives an H-beacon on channel k_1, it can make synchronization of frequency hopping with its cluster head on channel k_m in Ω_H at time $t_0 + (Mn + m - 1)T_{BI}$. Otherwise, it increases the beacon-loss counter $n_{rx,H}$ by one and then repeats the H-beacon reception process through the next hopping channel in Ω_H. If $n_{rx,H}$ reaches a threshold $\bar{n}_{rx,H}$, the child device becomes an orphan node and may need to initiate the network rejoining process.

When a child device does not receive an H-beacon on channel k, its beacon-loss counter n_{rx} will automatically reach $\bar{n}_{rx}$. Then, it searches for an H-beacon on channel k_1 in Ω_H. However, unlike in the former case, it does not know when the cluster head initiated the H-mode. It may need to search for the H-beacon for M times on each

channel in Ω_H, since the H-beacon is periodically transmitted at a period of MT_{BI} seconds on each channel in Ω_H. Once the child device receives an H-beacon, it can make synchronization of frequency hopping with the cluster head on channel k_j in Ω_H at time $t_0 + (Mn + j - 1)T_{BI}$, where $1 \le j \le M$. If not, it increases the counter $n_{rx,H}$ by one and then repeats the beacon reception process on the next hopping channel in Ω_H. If $n_{rx,H}$ reaches a threshold $\bar{n}_{rx,H}$, the child device becomes an orphan node and may need to initiate the network rejoining process.

Define the interference avoidance time by the time difference between when the cluster head transmits the channel hand-off command (i.e., H-beacon on channel k) and when the child device first receives an H-beacon in the H-mode. Let T_{IA} be the interference avoidance time of a child device that receives an H-beacon on channel k. Then, it can be shown that

$$\begin{aligned} T_{IA} &= (1-p_1)T_{BI} + p_1(1-p_2)2T_{BI} + \cdots + p_1 p_2 \cdots p_{\bar{n}_{rx,H}} \left[\left(\bar{n}_{rx,H} + 1 \right) T_{BI} + T_{RE} \right] \\ &= T_{BI} \left(1 + \sum_{i=1}^{\bar{n}_{rx,H}} \prod_{m=1}^{i} p_{k_{\mathrm{mod}(m-1,M)+1}} \right) + T_{RE} \prod_{m=1}^{\bar{n}_{rx,H}} p_{k_{\mathrm{mod}(m-1,M)+1}} \end{aligned} \tag{3.29}$$

where the subscript "mod" denotes the modulo operation and p_m denotes the failure probability of the m-th beacon transmission in the H-mode, given by

$$p_m = p_{k_{\mathrm{mod}(m-1,M)+1}}. \tag{3.30}$$

Let T'_{IA} be the avoidance time of a child device that does not receive an H-beacon on channel k. Then, it can be shown that

$$
\begin{aligned}
T'_{IA} &= T'_o + p_1(1-p_2)MT_{BI} + p_1p_2(1-p_3)2MT_{BI} \\
&\quad + \cdots + p_1p_2\cdots p_{\bar{n}_{rx,H}}\left(\bar{n}_{rx,H}MT_{BI} + T_{RE}\right) \\
&= \bar{n}_{rx}T_{BI} + MT_{BI}\sum_{i=1}^{\bar{n}_{rx,H}}\prod_{j=1}^{i}p_{k_{\mathrm{mod}(m-1,M)+1}} + T_{RE}\prod_{j=1}^{\bar{n}_{rx,H}}p_{k_{\mathrm{mod}(m-1,M)+1}}
\end{aligned}
\tag{3.31}
$$

where T'_o is the time difference between the beginning of the H-mode in the child device and the cluster head. Then, the average interference avoidance time $\bar{T}_{IA}$ can be represented as

$$
\begin{aligned}
\bar{T}_{IA} &= \left(1-p_{\mathrm{RTB},k}^{(N_b)}\right)T_{IA} + p_{\mathrm{RTB},k}^{(N_b)}T'_{IA} \\
&= \left\{T'_o + T_{BI}\left[(M-1)\sum_{i=1}^{\bar{n}_{rx,H}}\prod_{m=1}^{i}p_{k_{\mathrm{mod}(m-1,M)+1}} - 1\right]\right\}p_{\mathrm{RTB},k}^{(N_b)} \\
&\quad + T_{BI}\left(1+\sum_{i=1}^{\bar{n}_{rx,H}}\prod_{m=1}^{i}p_{k_{\mathrm{mod}(m-1,M)+1}}\right) + T_{RE}\prod_{m=1}^{\bar{n}_{rx,H}}p_{k_{\mathrm{mod}(m-1,M)+1}}.
\end{aligned}
\tag{3.32}
$$

It can be seen that the proposed RTB can reduce the failure probability of H-beacon delivery by a factor of $p_{\mathrm{RTB},k}^{(N_b)}$, contributing to significant reduction of the interference avoidance time.

The proposed scheme can determine the number of frequency hopping channels, M, and the set of frequency hopping channels, Ω_H, in consideration of the average synchronization time and the interference avoidance time. Assume that a child device is synchronized with its cluster head through channels in $\Omega = \{k_1, \ldots, k_M\}$ in the frequency hopping mode. Then, the average synchronization time T_Ω can be represented as

$$
\begin{aligned}
T_\Omega &= \left(1 - \frac{p_{k_1} + p_{k_2} + \cdots p_{k_M}}{M}\right)^{-1} T_{BI} \\
&= \frac{1}{1-p_\Omega}T_{BI}.
\end{aligned}
\tag{3.33}
$$

It can be seen that T_Ω dependes on the expeceted failure probability of beacon reception on channels in Ω (refer to Appendix A). Thus, it may be desirable to choose frequency hopping channels using a minimum number of uncorrelated channels that can minimize the average synchronization and the interference avoidance time as well.

We can reduce the probability p_Ω by choosing frequency hopping channels in consideration of major interference signal. When channel k is interfered by a wideband interferer, it is highly probable that its adjacent channels are also subject to the same interferer. Thus, we can choose frequency hopping channel k_m such that

$$|k_m - k| \geq \lfloor W/d \rfloor \tag{3.34}$$

where W denotes the bandwidth of the major interference signal. Considering the presence of plural interference sources, we can determine frequency hopping channels k_i and k_j in Ω such that

$$|k_i - k_j| \geq \lfloor W/d \rfloor \quad \text{for } 1 \leq i, j \leq M \quad i \neq j \tag{3.35}$$

where $M \geq 2$.

We can generate Q sets of frequency hopping channels satisfying (3.34) and (3.35). Let $\Omega(q)$ be the q-th set of frequency hopping channels, represented as

$$\Omega(q) = \{k_{1,q}, \cdots, k_{m,q}, \cdots, k_{M,q}\} \quad \text{for } q = 1, \cdots, Q \tag{3.36}$$

where $k_{m,q}$ denotes the index of the m-th channel in $\Omega(q)$. It may be desirable for a cluster head and its child devices to share the information on Ω without additional message exchanges among them. The frequency hopping channel set can be selected by

using a cluster key such as the cluster identifier or cluster head address. For example, the index of the hopping-channel set can be determined as

$$\hat{q} = 1 + \mathrm{mod}(ID, Q), \tag{3.37}$$

where ID denotes the cluster identifier.

For seamless channel hand-off, the cluster head evaluates the link quality of channels in Ω by measuring packet errors in the H-mode. For example, if it receives packets through channel k_m in Ω with the lowest PER, it may select channel k_m as the hand-off channel. Finally, all the devices in the same cluster use channel k_m when it is in turn for the signal transmission, while transmitting a normal beacon frame. In this way, the proposed scheme can rapidly avoid co-channel interference in a seamless manner.

The proposed RTB and H-mode may require information of 6 bits and 5 bits, respectively, which can be implemented simply using unused bits in the IEEE 802.15 beacon frame [2, 6]. This means that additional signaling overhead is not required. Moreover, the proposed scheme works in a cluster-wise manner, which means that the proposed scheme does not require for additional network-wide signaling. The proposed scheme can be applied to other low-power WSN technologies such as IEEE 802.11ah [52] and LoRa [53], which may operate by using periodic beaconing in unlicensed spectrum band.

3.4. Performance evaluation

We evaluate the performance of the proposed scheme by computer simulation and experiment as well. Fig. 3-4 illustrates network topologies for the evaluations. Fig. 3-4 (a)

and (b) illustrate an IEEE 802.15.4 cluster-tree network used for the evaluation in synthetic and real interference environments, respectively. Fig. 3-5 plots a screenshot of WLAN signal using a Wi-Fi Analyzer [54], illustrating the existence of plural WLANs. Table 3-1 summarizes the parameters for the evaluation environment of Fig. 3-4. We assume that all the IEEE 802.15.4 devices transmit signal by means of CSMA/CA with default MAC parameters suggested in the standardization. We design the proposed RTB to increase the number of repeated beacon transmissions by one in the absence of packet reception while satisfying the second constraint in (3.25), and to reduce it by one-half in the absence of delivery error in the past 10 beacon intervals. The beacon-loss threshold in the normal mode and H-mode is set to 8 and 6, respectively.

We implement the proposed scheme onto TelosB mote devices equipped with a Chipcon CC2420 radio transceiver [55]. The CC2420 radio transceiver can support a transmission rate of up to 250 Kbps in the 2.4GHz ISM band, while being fully compliant to the IEEE 802.15.4 PHY-layer. We use TKN15.4 [56], which is an open-source platform-independent IEEE 802.15.4-2006 MAC implementation for TinyOS 2.x. Table 3-2 summarizes memory overhead of the proposed scheme and conventional IEEE 802.15.4. Considering the usage of 48KB ROM and 10KB RAM in TelosB, it can be seen that the additional memory overhead for the proposed scheme is marginal. For the experiment in Fig. 3-4 (a) environments, netbooks equipped with IEEE 802.11 compliant NICs are used as Wi-Fi interferers, where D-ITG is used to generate Wi-Fi traffic at different rates [57].

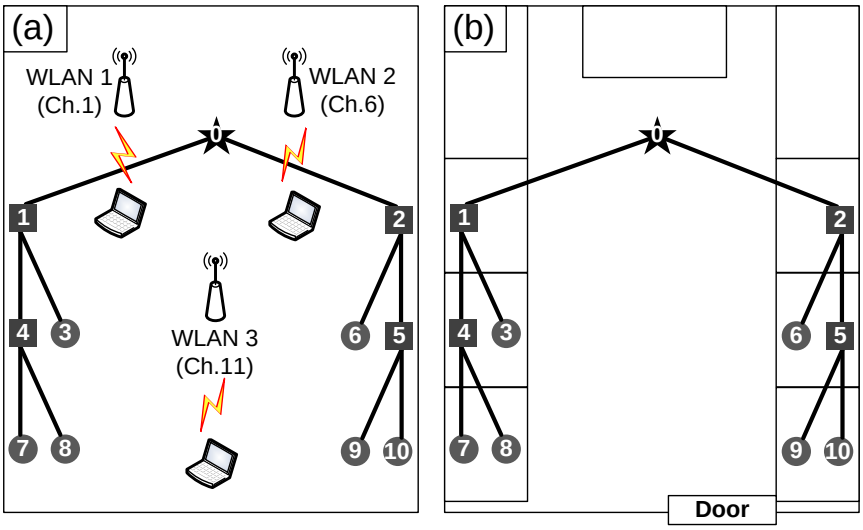

Fig. 3-4. Network topologies for performance evaluations.

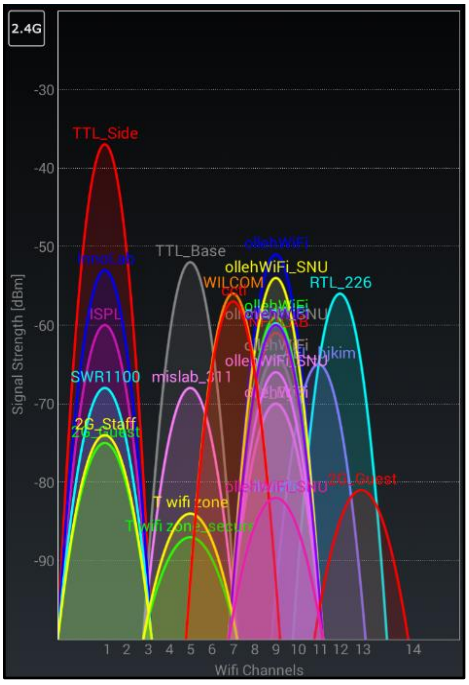

Fig. 3-5. A screenshot of WLAN signal obtained by Wi-Fi Analyzer.

Table 3-1. Evaluation parameters.

Parameters	Fig. 3-4 (a)	Fig. 3-4 (b)
Network topology	Cluster-tree (max. 3-hop)	
Beacon order/Super-frame order	6, 3	
Number of devices	10	
Traffic load of each device	1 packet/s	
Beacon frame length	40 bytes	
Data frame length	40 bytes	
Data frame buffer size	20	
Retransmission limit	3	
CSMA back-off limit	4	
Beacon synchronization limit	4	
Synchronization interval of non-tracking end device	30 min.	
Transmit power	0 dBm	
Number of hopping channels (Proposed)	4	
WLAN packet length	1 ms	Uncontrolled
WLAN idle state distribution	Exponential	
WLAN CCA type	Carrier sensing	
WLAN transmit power	17 dBm	

WLAN channel occupancy ratio	Varying	
Power consumption during Tx/Rx mode	70.0 mW, 78.3 mW	None
Power consumption in the idle/sleep mode	3.79 mW, 1.62 uW	

Table 3-2. Memory overhead on ROM and RAM.

	IEEE 802.15.4	Proposed scheme
ROM (program)	Cluster head: 26638 bytes Child device: 27070 bytes	Cluster head: + 1340 bytes (5.03%) Child device: + 688 bytes (2.54%)
RAM (data)	Cluster head: 1334 bytes Child device: 1450 bytes	Cluster head: + 48 bytes (3.59%) Child device: + 46 bytes (3.17%)

We also evaluate the performance of IEEE 802.15.4 PBM, IEEE 802.15.4e DBM and PRCH scheme for fair comparison. Fig. 3-6 through Fig. 3-8 plot the results in Fig. 3-4 (a) environment, where the network comprises one coordinator and 10 devices and (BO,SO) = (6,3). Each evaluation runs for 200 beacon intervals, where each device generates one data packet per second. We generate three IEEE 802.11g WLANs whose spectrum bands are not overlapped with each other, but at least one of which is overlapped with that of IEEE 802.15.4 signal. We assume that WLANs make their signal transmission between the 50-th and the 100-th beacon interval with a specified traffic load.

Fig. 3-6 (a) depicts the probability of successful beacon delivery according to the WLAN load. The solid and the dotted lines denote the simulation and the experiment results, respectively. It can be seen that both PBM and DBM seriously suffer from the presence of interference, and that DBM can provide marginal improvement over PBM

only when the interferer is located within a channel sensing range of the cluster head. It can also be seen that the proposed scheme provide high beacon delivery performance regardless of the cluster head position. This is mainly because the cluster head repeatedly transmits the beacon frame according to the channel condition and seamlessly changes the transmission channel in the presence of severe interference. It can also be seen that the simulation results quite agree well with the experiment results.

Fig. 3-6 (b) depicts the orphan probability according to the WLAN load. We assume that a child device becomes an orphan node when it does not receive a beacon frame four times consecutively. It can be seen that PBM and DBM suffer from a rapidly increasing number of orphan nodes as the WLAN load increases. This is mainly because it propagates the orphan state to all its descendant devices once a router device is orphaned from the network. It can also be seen that PRCH yields somewhat larger number of orphan nodes even when the WLAN load is low. This is mainly because the hand-off channel is determined without consideration of operating condition, yielding significant performance degradation in the presence of plural interference sources. It can also be seen that the proposed scheme is quite robust to the presence of WLAN interference. This result implies that the proposed scheme can robustly maintain the network operation even in harsh interference environments.

Fig. 3-7 depicts the data throughput when the WLAN load is 0.1 and 0.3, respectively. It can be seen that the IEEE 802.15.4 baseline is very susceptible to the presence of interference, but the proposed scheme is quite robust. It is mainly due to that the proposed scheme can fast avoid the co-channel interference by means of seamless channel-handoff

with the aid of reliable delivery of beacon signal. It can also be seen that the simulation agree well with the experiment results.

Fig. 3-8 (a) depicts the power consumption of routers and end devices according to the WLAN load. Two types of end devices in IEEE 802.15.4, tracking and non-tracking end device, have been considered [2]. The power consumption is measured for the beacon synchronization, data transmission/reception, processing during the active and the inactive period, and for the interference estimation in the proposed scheme. It can be seen that the power consumption of IEEE 802.15.4 end devices and routers significantly increases as the WLAN load increases, and that it becomes almost the same when the WLAN load is high. It can also be seen that the power consumption of the proposed scheme is little affected. This is mainly because the proposed scheme can remarkably reduce the orphan probability in addition to fast channel hand-off. The non-tracking end device may suffer from the increase of power consumption compared with the tracking end device in the presence of severe co-channel interference. This is mainly because in the case that a parent node has changed its operating channel, its non-tracking child nodes may not know in which channel its parent node is currently operating, increasing the synchronization time and power consumption. Note that the synchronization interval of the non-tracking end devices has been configured to 30 minutes.

Table 3-3 summarizes the power consumption of the proposed scheme when the WLAN load is 0, 0.2 and 0.4. Here, we set the synchronization interval of the non-tracking end devices to 1, 10 and 60 minutes. It can be seen that in the absence of the co-channel interference, the power consumption of the non-tracking end devices with 1 min-synchronization interval is lower than that of the tracking end devices. It can also be seen

that in the presence of the co-channel interference, however, the power consumption of the non-tracking end devices may exceed that of the tracking end devices. This result implies that the performance of the non-tracking end devices may be worse than that of the tracking end devices in the presence of co-channel interference unless the synchronization interval is set very long. It can be seen that if the synchronization interval is longer than 10 minutes, the power consumption of the non-tracking end devices may be kept lower than that of the tracking end devices even in the presence of co-channel interference.

Fig. 3-8 (b) depicts the cumulative distribution function (CDF) of the transmission delay from all devices to the coordinator when the WLAN load is 0.0 and 0.2. Note that the CDF does not converge to one even in the absence of interference because the transmission delay is measured using packets successfully delivered. That is, the value of Y-axis at the CDF end point represents the reliability of data transmission, which is defined by the ratio of the number of successfully received data packets and the total number of generated data packets. It can be seen that the proposed scheme can significantly reduce the transmission delay in addition to high transmission reliability. This is mainly because reliable reception of the beacon frame even in the presence of severe interference enables to maintain the network synchronization which is indispensable for the signal transmission.

Table 3-4 summarizes the transmission reliability when the WLAN load is 0.2 and 0.4. Here, ‘outage’ denotes the ratio of the number of dropped packets due to the connection failure (i.e., orphaned nodes) and the number of total generated packets, and ‘Tx. failure’ denotes the ratio of the number of dropped packets due to the failure

associated with channel access, retransmission and buffer overflow, and the number of total generated packets. It can be seen that PBM and DBM seriously suffer from the outage as the WLAN load increases. Note that the performance degradation is mainly due to the loss of network connectivity. It can also be seen that PRCH cannot provide desirable transmission reliability mainly due to unreliable channel hand-off, but the proposed scheme can provide transmission reliability quite robust to the presence of interference mainly due to timely channel hand-off with reliable transmission of beacon signal.

Fig. 3-9 depicts the performance in terms of the beacon delivery ratio, number of miss-connections and data delivery ratio in Fig. 3-4 (b) real environments, where the network comprises one coordinator and 10 devices and (*BO*,*SO*) = (6,3). The experiment has been conducted for a duration of 60 minutes and repeated 10 times in real interference environments where plural WLAN signals exist as shown in Fig. 3-5. It can be seen that the performance of IEEE 802.15.4 baseline is degraded even in normal operation environments. IEEE 802.15.4 baseline can improve data reliability by means of retransmissions, but it cannot improve beacon delivery performance. It implies that the IEEE 802.15.4 baseline may suffer from significant loss of synchronization. It can also be seen that the proposed scheme can successfully deliver the beacon at an average rate of 99.2% and also significantly improve the data delivery performance. This is mainly because the proposed scheme makes channel hand-off to the best one among the frequency hopping channels. Note that the performance of conventional ZigBee operating on channel 25 and 26 is good mainly due to low spectrum occupancy by WLANs as shown in Fig. 3-5.

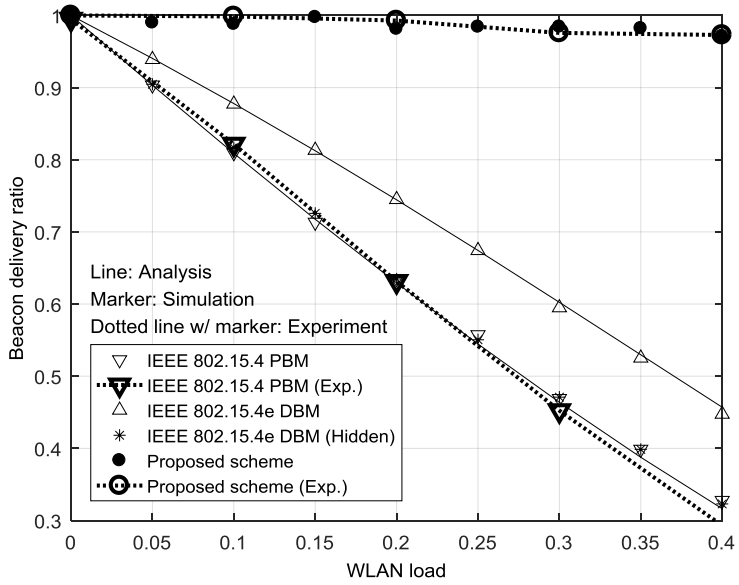

(a) Beacon delivery ratio.

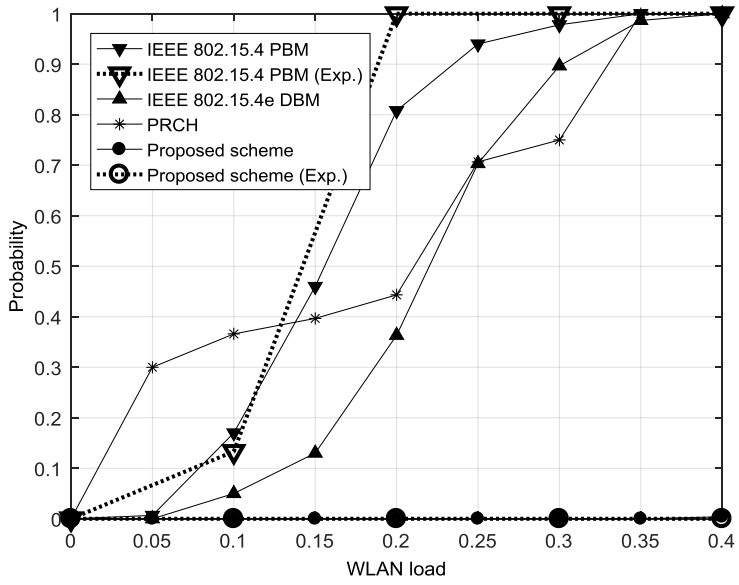

(b) Orphan probability.

Fig. 3-6. Connectivity performance according to the WLAN load.

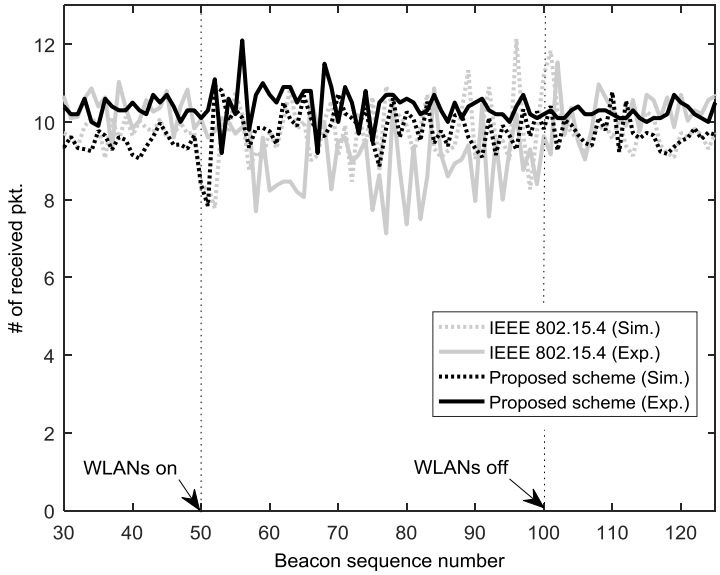

(a) When WLAN load is 0.1.

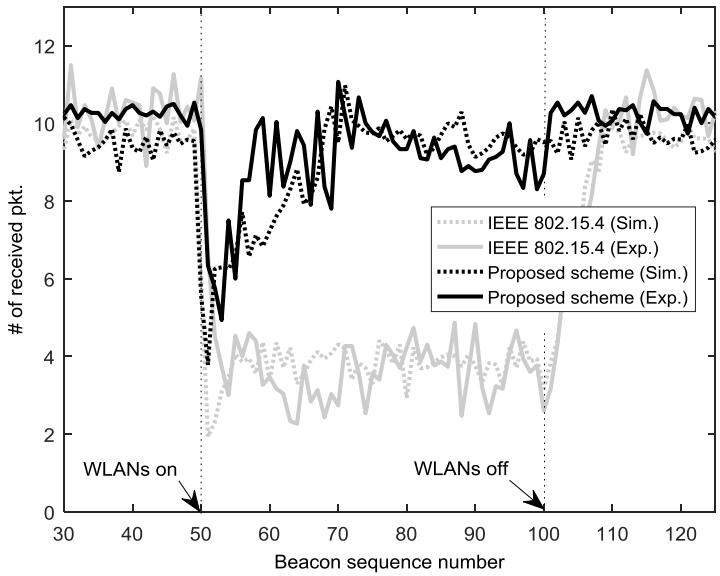

(b) When WLAN load is 0.3.

Fig. 3-7. Number of received packets according to the time.

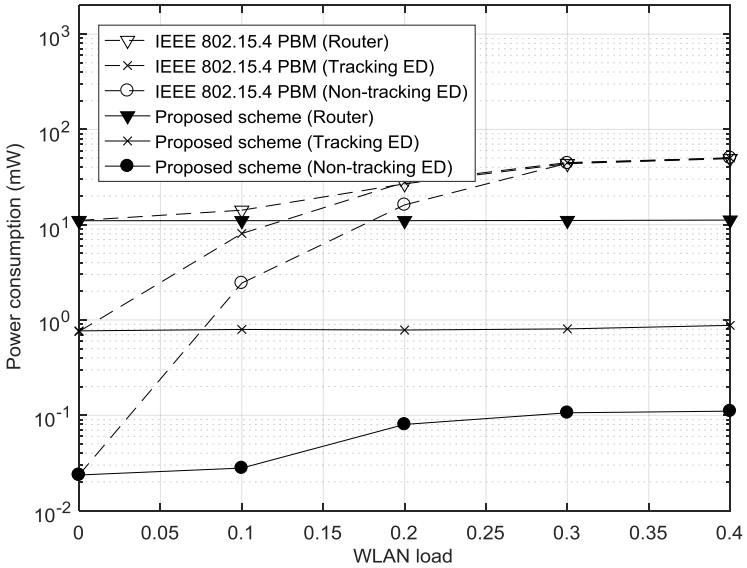

(a) Power consumption.

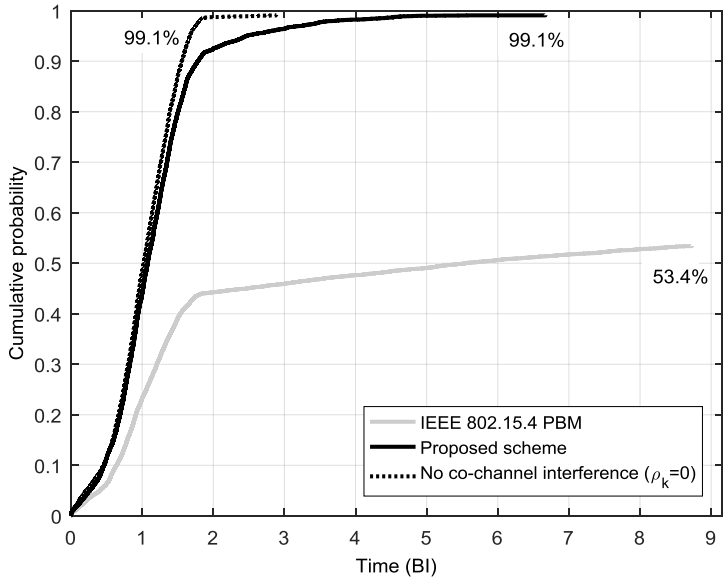

(b) Empirical CDF of delay when $\rho_k = 0$ and 0.2.

Fig. 3-8. Power consumption and transmission delay according to the WLAN load.

Table 3-3. Power consumption of the proposed scheme.

Unit: mW	$\rho_k = 0$	$\rho_k = 0.2$	$\rho_k = 0.4$
Router	11.0	11.02	11.18
Tracking end device	0.77	0.78	0.88
Non-tracking end device (Sync. interval: 1 min.)	0.66	2.29	3.14
Non-tracking end device (Sync. interval: 10 min.)	0.07	0.24	0.33
Non-tracking end device (Sync. interval: 60 min.)	0.01	0.04	0.06

Table 3-4. Reliability and transmission failure according to the WLAN.

Unit: %	$\rho_k = 0.2$			$\rho_k = 0.4$		
	Rel.	Tx. failure	Outage	Rel.	Tx. failure	Outage
IEEE 802.15.4 PBM	53.4	7.0	39.6	32.9	4.7	62.4
IEEE 802.15.4e DBM	68.1	6.3	25.6	45.2	4.9	49.9
PRCH	75.1	6.1	18.8	49.7	5.2	45.1
Proposed	99.1	0.9	0.0	94.6	5.4	0.0

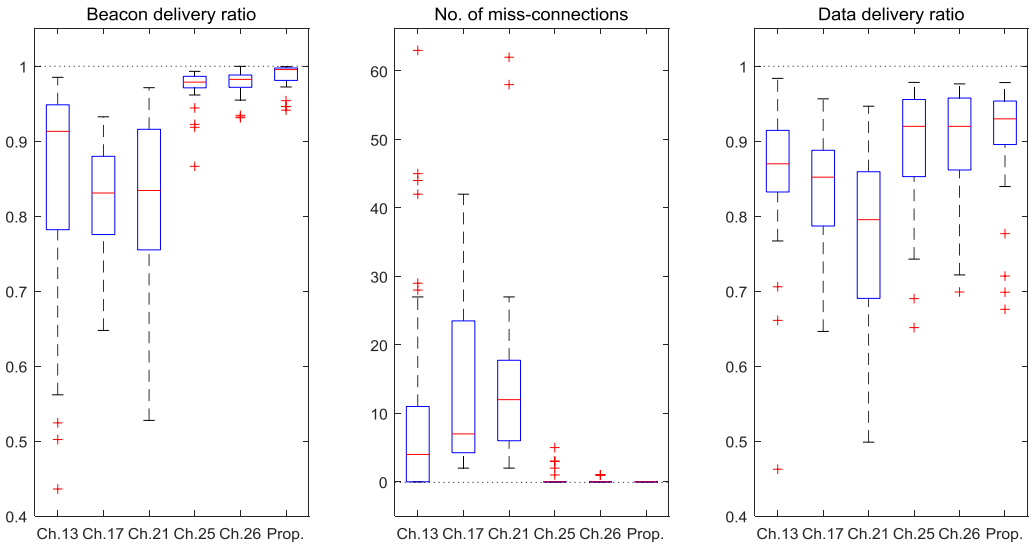

Fig. 3-9. Performance in real environments.

Chapter 4

Throughput maximization of low-power wireless sensor networks in interference environments

In this section, we consider the improvement of transmission performance of low-power WSNs by adjusting the transmission rate and the payload size according to the interference condition. We estimate the probability of transmission failure and the data throughput, and then determine the payload size to maximize the throughput performance. We investigate that the transmission time maximizing the normalized throughput is not much affected by the transmission rate, but rather by the interference condition. We independently adjust the transmission rate and the transmission time in response to the change of channel and interference condition, respectively. Finally, we verify the performance of the proposed scheme by computer simulation. The simulation results show that the proposed scheme significantly improves data throughput compared with conventional schemes while preserving energy efficiency even in the presence of interference.

4.1. System model

As illustrated in Fig. 4-1, we consider a star-topology WSN comprising a network coordinator and its child nodes located in an operation range of WLANs. The WSN employs a periodic frame structure for synchronous network operation and data communication, where the period of the frame and the length of the data communication interval are T_{period} and T_{comm}, respectively. The network coordinator transmits a beacon at the beginning of each frame for synchronized network operation. It allocates communication resource to a target node using a handshaking protocol during the network operation interval [2]. Non-target nodes may stay in a sleep mode to minimize power consumption.

We assume that a transmitter node generates L_{bulk}-bit data at each transaction. The L_{bulk}-bit data is fragmented by a number of data packets each of which comprises L-bit data payload ($L_{\min} \le L \le L_{\max}$) and signaling bits (e.g., packet header). The receiver confirms the packet reception by sending an ACK packet. The transmitter retransmits the data packet if it does not receive an ACK packet. We also assume that the transmission rate is adjustable according to the channel condition. Then, the packet transmission time with transmission mode m can be represented as

$$T_{\text{pkt},m}(L) = \frac{L_{\text{shr}} + L_{\text{phr}}}{R_{\text{base}}} + \frac{L_{\text{mhr}} + L}{R_m} \tag{4.1}$$

where L_{shr}, L_{phr} and L_{mhr} are respectively the bit size of the synchronization header (SHR), the physical layer packet header (PHR) and the medium access control (MAC) layer packet header (MHR), R_m ($\in \{R_1, R_2, ..., R_M\} \equiv \Pi$) denotes the transmission rate of

MHR and data payload of transmission mode m, and R_{base} is the transmission rate of SHR and PHR ($R_{\text{base}} \in \Pi$). We assume that $R_1 < R_2 < \cdots < R_M$ and the ACK packet has no payload (i.e., $L = 0$).

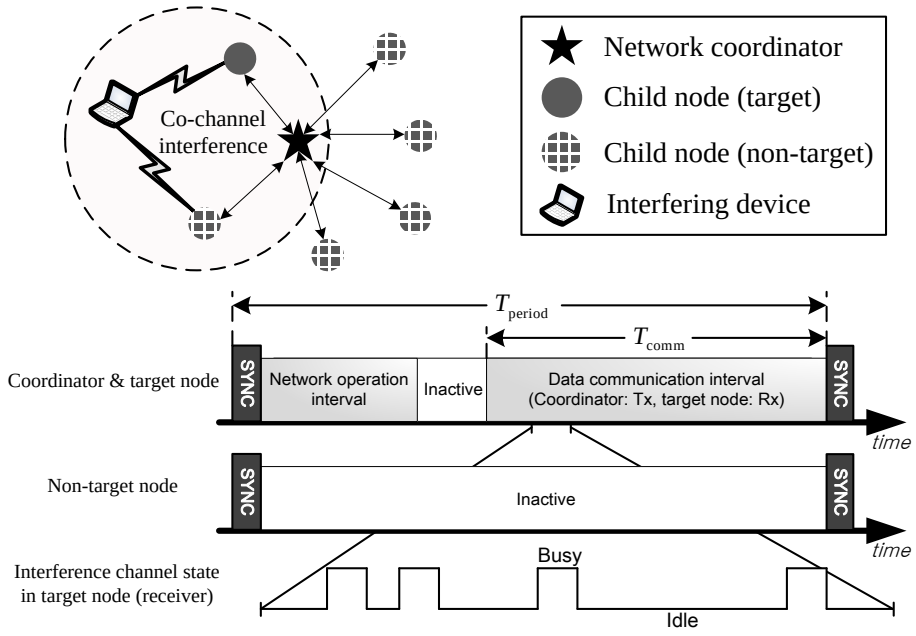

Fig. 4-1. A star-topology WSN in a synchronized operation mode.

A node with transmission mode *m* may experience packet loss when the received SNR, denoted by γ, is lower than a threshold $\hat{\gamma}_m$ and/or when the packet has collision with interference signal. We assume that the SNR is unchanged during each packet transmission and randomly varies between the packet transmissions [58]. Then, the probability of transmission failure can be represented as

$$\tilde{p}_m(L,\gamma) = 1-\left(1-p_{m,c}(L)\right)\left(1-p_{m,s}(L,\gamma)\right) \tag{4.2}$$

where $p_{m,c}$ and $p_{m,s}$ denote the probability of transmission failure due to the packet collision and low SNR, respectively. The probability of transmission failure due to SNR can be represented as

$$p_{m,s} = 1 - \left(1 - p_{\text{fail}}^{\text{sync}}(\gamma, L_{\text{shr}})\right)\left(1 - b_{m,s}(\gamma)\right)^{L_{\text{phr}} + L_{\text{mhr}}} \tag{4.3}$$

where $p_{\text{fail}}^{\text{sync}}(\gamma, L_{\text{shr}})$ denotes the probability of synchronization failure at an SNR of γ when the SHR length is L_{shr} (e.g., $p_{\text{fail}}^{\text{sync}}(\gamma, L_{\text{shr}})$ for IEEE 802.15.4 communications is referred in [59]), and $b_{m,s}(\gamma)$ denotes the BER of transmission mode m at an SNR of γ. Note that $\tilde{p}_m$ is an upper bound of the PER (refer to Appendix B).

The probability of transmission failure due to the packet collision can be calculated in terms of the channel occupancy of interference signal. The channel occupancy of WLAN signal can be characterized using a semi-Markov model [43, 44]. The channel has two simple operation states, busy and idle state, whose duration is described by the probability density function (PDF) $f_{T_{\text{busy}}}(t)$ and $f_{T_{\text{idle}}}(t)$, respectively. The channel occupancy of interference signal can be defined by

$$\rho = \frac{\tau_{\text{busy}}}{\tau_{\text{busy}} + \tau_{\text{idle}}} \tag{4.4}$$

where τ_{busy} and τ_{idle} denote the mean duration of the busy and the idle state, respectively. It can be shown that $p_{m,c}$ can be represented as

$$p_{m,c} = \rho\, p_{m,c|\text{busy}} + (1-\rho)\, p_{m,c|\text{idle}} \tag{4.5}$$

where $p_{m,c|\text{busy}}$ and $p_{m,c|\text{idle}}$ denote the probability of transmission failure due to the packet collision when the packet transmission is initiated in the presence and the absence

of interference signal, respectively. For a given probability of transmission failure, denoted by $\tilde{p}_{m,c}(L,\gamma)$, the data throughput can be represented as

$$S_m(L,\gamma) = \frac{L\left(1-\tilde{p}_{m,c}(L,\gamma)\right)}{\tilde{T}_m(L)} \text{ [bit/sec]} \tag{4.6}$$

where $\tilde{T}_m$ denotes the data transaction time (i.e., the round trip time).

Define the bulk transfer delay D_{bulk} by the sum of the access delay D_{acc} and the transmission delay D_{tx}. The access delay is the time difference between the start of an access attempt and the successful access. Then, it can be shown that

$$\begin{aligned} D_{\text{acc}} &= \frac{1}{2}T_{\text{period}} + \left(1-p_{\text{sync}}\right)\left(1-p_{\text{sch}}\right)T_{\text{period}} \\ &\quad + \left\{p_{\text{sync}} + \left(1-p_{\text{sync}}\right)p_{\text{sch}}\right\}\left(1-p_{\text{sch}}\right)\left(1-p_{\text{sync}}\right)2T_{\text{period}} + \cdots \\ &= \frac{1}{2}T_{\text{period}} + \frac{1}{\left(1-p_{\text{sync}}\right)\left(1-p_{\text{sch}}\right)}T_{\text{period}} \end{aligned} \tag{4.7}$$

where p_{sync} and p_{sch} denote the failure probability of the frame synchronization and the scheduling, respectively. Note that a low-power WSN can maintain the frame synchronization robust to the presence of co-channel interference with the use of the proposed scheme in Chapter 3. The transmission delay is the time difference between when the beginning of data transmission and the end of when it finishes all L_{bulk}-bit data transmissions. Then, it can be shown that

$$D_{\text{tx}} = \frac{1}{\left(1-p_{\text{sync}}\right)}\left\lceil \frac{L_{\text{bulk}}}{T_{\text{comm}}\bar{S}} \right\rceil T_{\text{period}} \tag{4.8}$$

where $\bar{S}$ denotes the average data throughput. We maximize the average data throughput of low-power WSNs in the presence of co-channel interference by adjusting the transmission rate and the payload size, minimizing the transmission delay.

4.2. Transmission in the presence of interference

We estimate the probability of transmission failure and data throughput in the presence of interference, and then determine the payload size maximizing the data throughput. We assume that a node transmits data packets without consideration of channel condition and confirms the transmission by receiving an ACK packet. The data transaction time can be represented as

$$\tilde{T}_m = T_{\text{pkt},m}^{data} + T_{\text{pkt},m}^{ack} + 2\delta \tag{4.9}$$

where $T_{\text{pkt},m}^{data} = T_{\text{pkt},m}(L)$, $T_{\text{pkt},m}^{ack} = T_{\text{pkt},m}(0)$, and δ denotes the time from the transmission to the reception state and vice versa. The probability of a transmission failure due to the packet collision can be represented as

$$p_{m,c} = 1 - \left(1 - p_{m,c}^{data}\right)\left(1 - p_{m,c}^{ack}\right) \tag{4.10}$$

where $p_{m,c}^{data}$ and $p_{m,c}^{ack}$ denote the collision probability of data and ACK packets, respectively.

When a data packet is transmitted in the presence of interference, it may experience the collision with a probability of one (i.e., $p_{m,c|\text{busy}} = 1$). Even when it is transmitted in the absence of interference, it may probabilistically experience the collision. Although a

WLAN device transmits signal after carrier sensing-based clear channel assessment (CCA) or energy-based CCA, it may not detect the presence of signal transmitted by low-power WSN devices. The probability of packet collision can be represented as

$$p_{m,c}^{data} = \begin{cases} \rho\ ; & \text{if interference source packet} \\ \rho + (1-\rho)\, p_{m,c|\text{idle}}^{data}; & \text{otherwise} \end{cases} \tag{4.11}$$

where $p_{m,c|\text{idle}}^{data}$ can be derived in what follows.

For given idle state length T_{idle} and data packet transmission time $T_{\text{pkt},m}^{data}$, a packet collision may occur if a data packet is transmitted $\left(T_{\text{idle}} - T_{\text{pkt},m}^{data}\right)$ seconds after the beginning of the idle state. Let t_d be the time difference between the beginning of the idle state and the presence of a new data packet (i.e., $0 \le t_d \le T_{\text{idle}}$). Assuming that the duration of the idle state is Pareto or exponentially distributed, it can be shown that

$$\begin{aligned} p_{m,c|\text{idle}}^{data}(t_d) &= \Pr\left[T_{\text{idle}} < t_d + T_{\text{pkt},m}^{data} \mid t_d\right] \\ &= \begin{cases} 1 - \left(\dfrac{t_d}{t_d + T_{\text{pkt},m}^{data}}\right)^{\sigma} & ; \quad \text{Pareto dis} \\ 1 - \exp\left(-\tau_{\text{idle}}^{-1} T_{\text{pkt},m}^{data}\right) & ; \quad \text{expo} \end{cases} \end{aligned} \tag{4.12}$$

where σ denotes the shape parameter of Pareto distribution. It can be seen that the probability depends on t_d when the idle state is Pareto-distributed. When the idle state is exponentially distributed, (4.11) can be rewritten as

$$p_{m,c}^{data} = \begin{cases} \rho & ; \quad \text{when interference source packet} \\ 1 - (1-\rho)\, \exp\left(-\tau_{\text{idle}}^{-1} T_{\text{pkt},m}^{data}\right) & ; \quad \text{oth} \end{cases} \tag{4.13}$$

Similarly, it can be shown that the collision probability of an ACK packet after successful data packet transmission can be represented as

$$p_{m,c}^{ack} = 1 - \exp\left(-\tau_{idle}^{-1}\left(\delta + T_{mhr}^{ack}\right)\right). \tag{4.14}$$

The probability of transmission failure due to the packet collision can be represented as

$$p_{m,c}(L) = 1 - (1-\rho)\exp\left(-\frac{L+\alpha_m}{R_m \tau_{idle}}\right) \tag{4.15}$$

where α_m is a constant indifferent from the payload size L and can be determined as

$$\begin{aligned}\alpha_m &= \alpha'_m R_m \\ &= \left(2T_{base} + \frac{L_{mhr}^{data} + L_{mhr}^{ack}}{R_m} + \delta\right) R_m.\end{aligned} \tag{4.16}$$

Here, $T_{base} = \left(L_{shr} + L_{phr}\right)/R_{base}$, and L_{mhr}^{data} and L_{mhr}^{ack} respectively denote the MHR bit size of data and ACK packet.

It can be shown that the data throughput can be represented as

$$\begin{aligned}S_m(L,\gamma) = R_m \frac{L}{L+\beta_m}(1-\rho)\exp\left(-\frac{L+\alpha_m}{R_m \tau_{idle}}\right) \\ \times\left(1-b_{base,s}(\gamma_s)\right)^{L_{phr}^{data}+L_{mhr}^{ack}}\left(1-b_{m,s}(\gamma_s)\right)^{L+L^{data}+L_{mhr}^{ack}}\end{aligned} \tag{4.17}$$

where $\beta_m = \beta'_m R_m = \left(\alpha'_m + \delta\right) R_m$ and $b_{base,s}$ denotes the BER of PHR transmission. Assuming that $b_{base,s}$ and $b_{m,s}$ are very low with the use of an appropriate transmission rate in the absence of interference, (4.17) can be approximated as

$$S_m(L,\gamma) \approx R_m \frac{L}{L+\beta_m}(1-\rho)\exp\left(-\frac{L+\alpha_m}{R_m \tau_{idle}}\right). \tag{4.18}$$

Taking the derivative of (4.18) with respect to L, i.e.,

$$\frac{\partial S_m}{\partial L} = -\frac{\tau_{\text{idle}}^{-1}(1-\rho)}{(L+\beta_m)^2}\exp\left(-\frac{L+\alpha_m}{R_m\tau_{\text{idle}}}\right)\left(L^2+\beta_m L-\beta_m R_m\tau_{\text{idle}}\right). \tag{4.19}$$

we can see that there exists a payload size that maximizes the data throughput. This implies a tradeoff between the packet transmission efficiency and the probability of transmission failure. The use of a smaller payload size may improve the robustness to interference, but it may also increase the signaling overhead, deteriorating the overall transmission efficiency.

The payload size maximizing the data throughput can be determined as

$$L_m^* \cong -\frac{\beta_m}{2}+\sqrt{\left(\frac{\beta_m}{2}\right)^2+\beta_m R_m\tau_{\text{idle}}}. \tag{4.20}$$

It can be seen that the payload size depends on the average idle period of interference, τ_{idle}, and the transmission rate R_m as well. With $\beta_m = \beta_m' R_m$, (4.20) can be rewritten as

$$\begin{aligned} L_m^* &= \left[-\frac{\beta_m'}{2}+\sqrt{\left(\frac{\beta_m'}{2}\right)^2+\beta_m'\tau_{\text{idle}}}\right]R_m \\ &= T_m^* R_m \end{aligned} \tag{4.21}$$

where T_m^* denotes the payload transmission time that maximizes the data throughput. It can be shown that

$$\frac{\partial L_m^*}{\partial R_m} = T_m^* + R_m\frac{\partial T_m^*}{\partial R_m} >> \frac{\partial T_m^*}{\partial R_m}. \tag{4.22}$$

Since R_m is typically large, (4.22) implies that the sensitivity of the payload transmission time with respect to the transmission rate is much smaller than that of the payload size. Moreover, T_m^* depends on β_m'. The sensitivity of β_m' with respect to the

transmission rate is much smaller than that of β_m. The transmission time can approximately be represented as

$$T_m^* \cong -\frac{\beta}{2} + \sqrt{\left(\frac{\beta}{2}\right)^2 + \beta\tau_{\text{idl}}} \\ = T^*. \tag{4.23}$$

It can be seen that T^* depends on τ_{idle} and not on the transmission rate. Note that the payload size L_m^* depends on the transmission rate.

4.3. Proposed transmission scheme

Exploiting the above investigation, we consider performance improvement of low-power WSNs in the presence of interference. We determine the initial payload size based on the interference characteristics estimated by (4.20). Exploiting (4.23), we adjust the transmission rate R and the transmission time T in response to the change of channel and interference condition, respectively. Algorithm 4-I summarizes the proposed scheme.

We initially determine the payload size by estimating the average idle period of interference. We define the interference estimation interval by the dedicated interval within the first data communication interval of a pair of scheduled nodes. With the use of an energy-type detector for the channel sensing, the transmitter node can estimate the channel occupancy of interference signal as

$$\tilde{\rho} = \frac{1}{N_s}\sum_{j=1}^{N_s} I\{y_j > \lambda\} \tag{4.24}$$

where $I\{\cdot\}$ is an indicator function, y_j is the energy of the j-th received sample, λ is a threshold level and N_s is the total number of samples for the measurement. It can be shown that the average busy period of interference can be estimated as

$$\tilde{\tau}_{\text{busy}} = \frac{1}{N_{\text{busy}}} \sum_{j=1}^{N_{\text{busy}}} n_{\text{busy},j} T_s \tag{4.25}$$

where N_{busy} is the number of busy periods, $n_{\text{busy},j}$ is the length of the j-th busy period and T_s is the channel sensing interval. Finally, the average idle period of interference can be estimated as

$$\tilde{\tau}_{\text{idle}} = \tilde{\tau}_{\text{busy}} \left(\frac{1}{\tilde{\rho}} - 1 \right). \tag{4.26}$$

As an example, when $N_s = 10$ and $T_s = 320\text{us}$, assume that the result of channel sensing is {O,O,X,X,X,O,X,X,X,X}, where “O” and “X” denote the presence and the absence of interference, respectively. Then, it is estimated that the channel occupancy of interference signal is 0.3, the average busy period of interference is 480 us, and the average idle period of interference is 1.12 ms, since $N_{\text{busy}} = 2$, $n_{\text{busy},1} = 2$ and $n_{\text{busy},2} = 1$. The initial payload size can be determined as

$$L_{\text{init}} = -\frac{\beta_m}{2} + \sqrt{\left(\frac{\beta_m}{2}\right)^2 + \beta_m R_m \tilde{\tau}_{\text{idle}}} \tag{4.27}$$

where the initial transmission rate can independently be determined in what follows.

The transmitter node determines the transmission rate based on the estimated SNR. It determines the transmission rate of the next data packet based on the received signal strength (RSS) of the ACK packet received most recently. It can determine the initial

transmission rate from the RSS of received packets. For an estimated SNR $\tilde{\gamma}$, it determines the transmission rate by the highest transmission rate R_m that satisfies $\tilde{\gamma} \geq \hat{\gamma}_m$, where $\hat{\gamma}_m$ is the minimum SNR for transmission mode m, which can provide desired PER of p_s with the use of maximum payload size in the absence of interference and can be represented as

$$\hat{\gamma}_m = b_{m,s}^{-1}\left(1 - p_s^{1/L_{m,a}}\right). \tag{4.28}$$

Here $b_{m,s}^{-1}$ denotes the inverse function of $b_{m,s}$. As described in Section 4.1, the packet loss can occur due to low SNR and/or packet collision. If the packet loss is mainly due to low SNR, it may be desirable to decrease the transmission rate R. If it is mainly due to the packet collision, it may be desirable to decrease the transmission time T to reduce the collision probability.

Consider the case that the transmission failure consecutively occurs due to the packet collision and the transmitter node decreases the transmission rate. Then, the transmission time will be increased and thus the packet collision problem may rather be exacerbated. This problem can be alleviated by adjusting the transmission rate and the transmission time together. If the number of consecutive transmission failures reaches a threshold N_{fail}, the transmitter node reduces the transmission rate, while keeping the transmission time T unchanged. If the transmission rate is adjusted from R_a to R_b, it may be desirable to adjust the payload size from L_a to L_b as

$$L_b = R_b T = R_b\left(\frac{L_a}{R_a}\right). \tag{4.29}$$

It may be feasible for the transmitter node to adjust the transmission time T according to the interference condition, while adjusting the transmission rate according to the channel condition. The normalized throughput, defined by $\tilde{S} = S_m / R_m$, can be estimated by

$$\tilde{S} = \frac{T}{T+\beta'} \sum_{i=1}^{W} I\{\text{ACK packet is received for packet } i\} \qquad (4.30)$$

after performance measurement of W-packet transmission. Note that this metric is not affected by the adjustment of transmission rate since it is normalized with respect to the transmission rate. After each W-packet transmission, the transmitter node updates the normalized throughput, say $\tilde{S}_{\text{new}}$. Comparing $\tilde{S}_{\text{new}}$ with a previous one, say $\tilde{S}_{\text{old}}$, it can adjust the transmission time T to increase the normalized throughput. Let Δ be the step size for the adjustment of transmission time and I_T $(=\pm 1)$ be a parameter indicating whether the transmission time was increased or decreased previously. If $\tilde{S}_{\text{new}} > \eta \tilde{S}_{\text{old}}$, where $\eta \geq 1$, it implies that the transmission time was effectively adjusted. In this case, it may be desirable to keep the adjustment. The transmitter node increases or decreases the transmission time by Δ according to I_T. If $\tilde{S}_{\text{old}} > \eta \tilde{S}_{\text{new}}$, it implies that the previous adjustment was not effective, requiring the change of the sign of I_T (i.e., $I_T \leftarrow -I_T$). Then, the transmitter node adjusts the transmission time by $I_T \Delta$. Otherwise, the transmitter node does not adjust the transmission time. It may also be desirable to change the step size in consideration of the difference between $\tilde{S}_{\text{new}}$ and $\tilde{S}_{\text{old}}$. If the difference is large, it may be desirable to use a larger step size to fast adjust the transmission time. It may also be desirable to employ channel sensing to fast adjust the transmission time. Algorithm 4-II summarizes the adjustment of the transmission time.

Algorithm 4-I. Overall process of the proposed scheme.

Initialize $R \leftarrow R_{\text{init}}$ using $\tilde{\gamma}$

Initialize $L \leftarrow L_{\text{init}}$ using $\tilde{\tau}_{\text{idle}}$ and R

$L \leftarrow \text{median}\left(L_{\min}, L, L_{\max}\right)$

$T \leftarrow L/R$

Initialize $I_T \leftarrow 1$ and $\tilde{S}_{\text{new}}, \tilde{S}_{\text{old}} \leftarrow 0$

while L_{bulk} -bit data is not delivered **do**

  for $i = 1:W$ **do**

    Transmit a data packet with R and L

    if an ACK packet is received **then**

      $n_{\text{fail}} \leftarrow 0$

      $\tilde{S}_{\text{new}} \leftarrow \tilde{S}_{\text{new}} + T/\left(T + \beta'\right)$

      Update R using $\tilde{\gamma}$

      $L \leftarrow \text{median}\left(L_{\min}, RT, L_{\max}\right)$

      $T \leftarrow L/R$

    else

      n_{fail} ++

      if $n_{\text{fail}} > N_{\text{fail}}$ **then**

        $R \leftarrow R_1$

        $L \leftarrow \text{median}\left(L_{\min}, RT, L_{\max}\right)$

        $T \leftarrow L/R$

      end if

    end if

  end for

  Update T by **Algorithm 4-II**

  $L \leftarrow \text{median}\left(L_{\min}, RT, L_{\max}\right)$

  $T \leftarrow L/R$

end while

Algorithm 4-II. Adjustment of transmission time.

If $\tilde{S}_{\text{new}} > \tilde{S}_{\text{old}} > 0$ **then**
  If $\tilde{S}_{\text{new}} > \eta_1 \tilde{S}_{\text{old}}$ **then**
    $T \leftarrow \Delta_1^{I_T} T$
  else if $\tilde{S}_{\text{new}} > \eta_2 \tilde{S}_{\text{old}}$ **then**
    $T \leftarrow T + I_T \Delta_2$
  end if
else
  If $\tilde{S}_{\text{old}} > \eta_1 \tilde{S}_{\text{new}}$ **then**
    $T \leftarrow \Delta_1^{-I_T} T$
  else if $\tilde{S}_{\text{old}} > \eta_2 \tilde{S}_{\text{new}}$ **then**
    $T \leftarrow T - I_T \Delta_2$
  end if
  $I_T \leftarrow -I_T$
end if
$\tilde{S}_{\text{old}} \leftarrow \tilde{S}_{\text{new}}$ and $\tilde{S}_{\text{new}} \leftarrow 0$

The proposed scheme can directly be applied to IEEE 802.15.4e DSME MAC [42] and 15.4g PHY [60] based WSNs. It can also be applied to tree or mesh topology with an appropriate link scheduling scheme that can provide robustness to collision between multiple communication links [61, 62].

4.4. Performance evaluation

We evaluate the performance of the proposed scheme by computer simulation using a lab-developed WSN simulator written in C++. Fig. 4-2 depicts the simulator structure,

which considers data transmission from the network coordinator to its child nodes in the presence of IEEE 802.11g WLAN interference signals [43, 44] in Ricean fading channel with a maximum Doppler frequency of f_D [58]. For the performance evaluation, we use Monte Carlo simulations of 300 iterations, each of which runs 1.5×10^5 simulation time slots.

The simulation environment is summarized in Table 4-1, which is mainly based on the specification of the IEEE 802.15.4 PHY layer. For comparison, we also consider the performance of seven schemes; an IEEE 802.15.4 baseline scheme at a transmission rate of 250 Kbps with a fixed payload size, DRACER that adjusts the transmission rate with a fixed payload size [31], DPLC that adjusts the payload size at a fixed transmission rate of 250 Kbps [32], DRACER with DPLC that adjusts the transmission rate and the payload size by using DRACER and DPLC, respectively, a streaming datalink layer scheme which is a static PPR scheme referred to Seda [34], a hybrid frame fragmentation scheme which is a dynamic PPR scheme referred to HiFrag [36], and a green frame fragmentation scheme which is a combination of HiFrag and transmit power adaptation referred to GreenFrag [37]. The proposed scheme and DRACER use one of four transmission rates, 250, 500, 1000 and 2000 Kbps, by adjusting the spreading factor with an appropriate coding set, while using the same spectrum bandwidth as conventional IEEE 802.15.4 [31, 63, 64]. The transmission rate can be informed to the receiver using a start frame delimiter (SFD) without additional signaling overhead [31]. Considering application areas of WSNs, we assume that the maximum payload size is 1024 bytes, which is larger than that of conventional IEEE 802.15.4 PHY layer (i.e., 127 bytes). Note that IEEE 802.15.4g, a recent amendment of IEEE 802.15.4, supports a maximum

payload size of up to 2047 bytes with using almost the same PHY layer techniques as IEEE 802.15.4 [60].

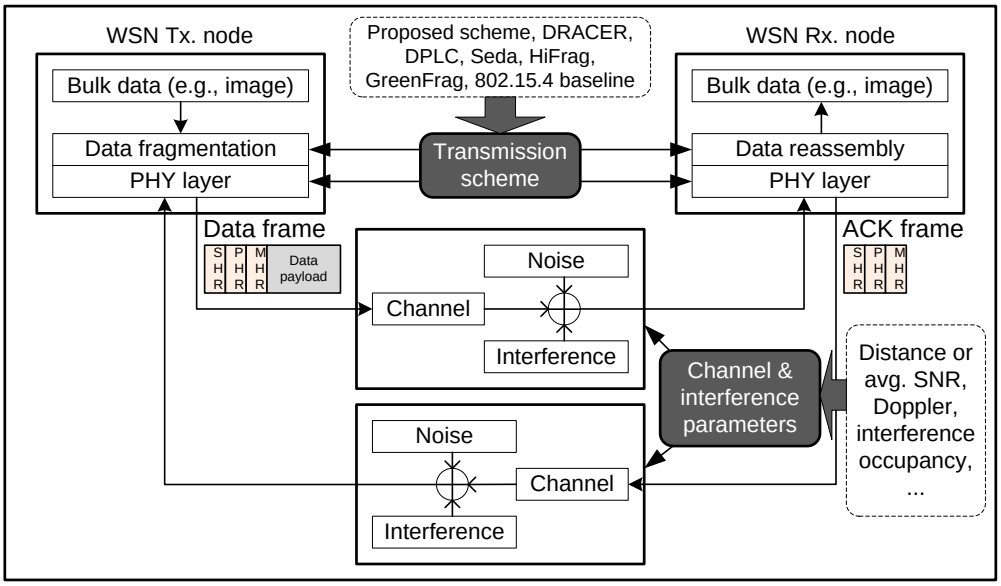

Fig. 4-2. WSN simulator structure.

Table 4-1. Evaluation parameters.

Parameters	Values
L_{shr}	5 bytes
L_{phr}	1 byte
R_{base}	250 Kbps
$L_{\text{uhr}}^{data}, L_{\text{uhr}}^{ack}$	9, 5 bytes
R	250, 500, 1000, 2000 Kbps [63]
Path loss model	Indoor channel model [2]

Transmit power	0 dBm
δ	192 us
T_s	320 us
L_{bulk}	65 Kbytes
P_{tx}, P_{rx}, P_{idle}	49.9, 56.5, 1.2 mW [35]
N_{fail}	3
η_1, η_2	1.2, 1.2
Δ_1, Δ_2	2, 320 us
W	10
$L_{\text{min}}, L_{\text{max}}$	20, 1024 bytes
T_{period}	983.04 ms
T_{comm}	491.52 ms
Simulation time slot	40 us
f_D	0.1 Hz
WLAN packet length (τ_{busy})	2 ms
WLAN idle state distribution	Exponential
WLAN CCA type	Carrier sensing
WLAN transmit power	17 dBm

Fig. 4-3 depicts the data throughput according to data payload size when the channel occupancy of interference signal ρ, is 0 and 0.2. The error bar represents the standard deviation of simulation result. To observe the impact of the channel occupancy of interference signal on the performance, we assume that $f_D = 0$ Hz. We also assume that the SNR is high enough so that the transmitter can employ all the transmission rates. It can be seen that when $\rho = 0$, the data throughput increases indifferently from the transmission rate as the payload size increases, which is mainly due to the decrease of the header signaling overhead. When $\rho = 0.2$, however, there exists a payload size maximizing the data throughput at each transmission rate. It is mainly due to the fact that the use of a larger payload size may become more susceptible to the collision. It can also be seen that the analytic results agree very well with the simulation results.

Fig. 4-4 depicts the energy consumption (in uJoule/bit) of WSN transmitter and receiver according to the data payload size when $\rho = 0$ and 0.2, which is measured from power consumption for transmission and reception of all packets, and power consumption during idle listening (i.e., waiting a packet) as well. It can be seen that when $\rho = 0$, the energy consumption somewhat decreases as the payload size increases mainly due to the increase of the throughput. Note that the energy consumption $E\left(= P_{avg}/S\right)$ may increase as the payload size increases, where P_{avg} denotes the average power consumption. When $\rho = 0.2$, however, there exists a payload size that minimizes the energy consumption, which is slightly different from one that maximizes the throughput. This is mainly due to the fact that P_{avg} varies with the payload size. It can also be seen that the use of higher transmission rate considerably reduces the power consumption, implying that the transmission rate should be adjusted according to the channel condition.

Fig. 4-5 depicts the normalized throughput according to the transmission time. It can be seen that the normalized throughput and the optimum transmission time are quite affected by the channel occupancy of interference signal, but little by the transmission rate. Note that the data throughput and the optimum payload size depend on the transmission rate. This property makes it desirable to adjust the transmission time according to the interference condition and the transmission rate according to the channel condition.

Fig. 4-6 depicts the data throughput according to the channel occupancy of interference signal when the SNR is 8 dB and the maximum Doppler frequency is 0.1 Hz, where the IEEE 802.15.4 baseline and DRACER use a fixed payload size of 300 or 1000 bytes, DPLC uses an initial payload size of 300 or 1000 bytes and adjusts it according to the performance, and Seda, HiFrag and GreenFrag use their own frame structure proposed in their works, whereas the proposed scheme determines the initial payload size by estimating the average idle period of interference and then adjusts it according to the throughput performance. We also evaluate the performance of the proposed scheme with channel hand-off scheme in Chapter 3. It can be seen that the IEEE 802.15.4 baseline provides very poor throughput performance even with the use of a large payload size (i.e., 300 or 1000 bytes) mainly due to the use of a low fixed transmission rate. It can also be seen that DRACER can improve the throughput performance by adjusting the transmission rate, but it may suffer from performance degradation with the use of a small fixed payload size in the absence of interference, which is mainly due to the transmission inefficiency, or with the use of a large fixed payload size in the presence of interference, which is mainly due to the increase of packet collision. We consider two DRACER

schemes; DRACER I that transmits packets at the highest rate regardless of transmission failure and DRACER II that adjusts the transmission rate in response to transmission failure. It was reported that these schemes are effective in interference and channel fading environment, respectively [31]. However, it can be seen that DRACER I and II make little difference on the transmission performance. This is mainly because they do not consider the effect of the payload size in the presence of interference, yielding inefficient use of white space. It can also be seen that DPLC can little improve the throughput performance even with the use of DRACER. This is mainly because it does not consider the effect of the transmission rate adjustment with a fixed step size of 10 bytes regardless of the transmission rate [32], yielding inefficient use of white space and slow adaptation of the payload size. It can also be seen that the proposed scheme significantly outperforms the other schemes by adjusting both the transmission rate and the transmission time in response to the change of interference and channel condition. It can also be seen that the proposed scheme with channel hand-off remarkably outperforms the proposed scheme by fast avoiding the effect of the co-channel interference. It can also be seen that the PPR schemes (i.e., Seda, HiFrag and GreenFrag) may provide throughput improvement over the IEEE 802.15.4 baseline in the presence of co-channel interference. This is mainly because they partition the data packet into a number of small blocks and adapt the block size based on the transmission performance, which may provide robustness to co-channel interference. It can also be seen that they may outperform DPLC, which is mainly due to fast adaptation of the block size. However, PPR schemes may severely suffer from the presence of co-channel interference, mainly due to frequent loss of recovery frame. It can also be seen that their performance are limited mainly due to the

use of a low fixed transmission rate, fixed frame structure and small maximum payload size. It may not be easy for the PPR schemes to increase the maximum payload size and the transmission rate since the computational complexity may considerably increase as the number of blocks for the packet partitioning increases.

Fig. 4-7 depicts the throughput according to the SNR when $\rho = 0$ and 0.2. Since DPLC does not provide noticeable performance improvement over the IEEE 802.15.4 baseline and DRACER, we hereafter consider the performance of the IEEE 802.15.4 baseline and DRACER for clarity of description. It can be seen that DRACER can improve the performance of the IEEE 802.15.4 baseline by using a large payload size in the absence of interference and a small payload size in the presence of interference. However, there is no proposed strategy when to employ DRACER I and II, and how to adjust the payload size together in the presence of interference and channel fading. It can also be seen that the proposed scheme can significantly improve the throughput performance by independently adjusting the transmission rate and the transmission time according to interference characteristics and channel condition, respectively. It can be seen that GreenFrag provides poorer throughput performance than HiFrag although GreenFrag is a combination of HiFrag and transmit power adaptation, where it uses a transmit power level of 0, -3, -7, -15 or -25 dBm. When GreenFrag confirms good transmission performance, it reduces the transmit power without consideration of channel condition. This may cause a ping-pong effect, seriously deteriorating the throughput performance. In fact, GreenFrag may not work well unless the SNR is sufficiently high (e.g., > 30 dB).

Fig. 4-8 depicts the energy consumption (in uJoule/bit) according to the SNR when $\rho = 0$ and 0.2. The power consumption of GreenFrag is measured at various power levels [37]. It can be seen that the power consumption increases when the SNR decreases or the channel occupancy of interference signal increases, which is mainly due to the increase of transmission failure. It can also be seen that the proposed scheme reduces the power consumption by adjusting the transmission rate and the transmission time. However, the gain in power consumption is somewhat marginal. It is mainly because the use of a larger payload size in the absence of interference may increase the data throughput and the average power consumption as well.

Table 4-2 summarizes the transmission delay according to the SNR when $\rho = 0$ and 0.2, where $T_{\text{period}} = 983.04$ ms, $T_{\text{comm}} = 0.5T_{\text{period}}$ and $L_{\text{bulk}} = 65$ Kbytes. It can be seen that the transmission delay decreases when the SNR increases or the channel occupancy of interference signal decreases, which is mainly due to the increase of data throughput. It can also be seen that the proposed scheme and DRACER significantly outperform the other schemes, which is mainly due to the transmission rate adjustment. It can also be seen that the proposed scheme can reduce the transmission delay further than DRACER both in the absence and the presence of interference. It is mainly because the proposed scheme can adjust both the transmission rate and the payload size to maximize the data throughput in response to the change of operation environments.

Fig. 4-9 (b) and (c) depicts the throughput in the presence of interference signal with $\rho = 0.2$ and a mobility of 3 Km/hour as illustrated in Fig. 4-9 (a), where the SNR slowly changes with a value of 35 ~ 40 dB, but the SINR changes from -20 to 20 dB when the maximum transmission rate is limited to 2 Mbps and 250 Kbps, respectively. It can be

seen that the throughput performance is severely affected by the position between the interference source and the WSN receiver, which is mainly due to the change of SINR. Fig. 4-9 (b) depicts the performance of the proposed scheme and DRACER since they outperform the other schemes. It can be seen that DRACER I outperforms DRACER II, which is mainly because it keeps the highest rate indifferently from transmission failure. When the SNR is not high enough to employ the highest rate, however, DRACER I may not outperform DRACER II (as shown in Fig. 7). It can also be seen that the proposed scheme outperforms DRACER I and II by adjusting both the transmission rate and the payload size, maximally exploiting the white space of interference signal. The performance gap between the proposed scheme and DRACER I increases as the SNR decreases. Fig. 4-9 (c) depicts the performance of the proposed scheme without adjustment of transmission rate, DPLC and the PPR schemes. It can be seen from Fig. 4-9 (c) that DPLC provides poor throughput performance, which is mainly due to slow adaptation of the payload size. It can also be seen that the performance of PPR schemes is limited mainly due to the use of a fixed frame structure and small maximum payload size. It can also be seen that the proposed scheme outperforms the other schemes, which is mainly due to fast adaptation of the payload size with a large maximum payload size. Note that it may not be easy for the PPR schemes to increase the maximum payload size since the computational complexity may considerably increase as the number of blocks for the packet partitioning increases.

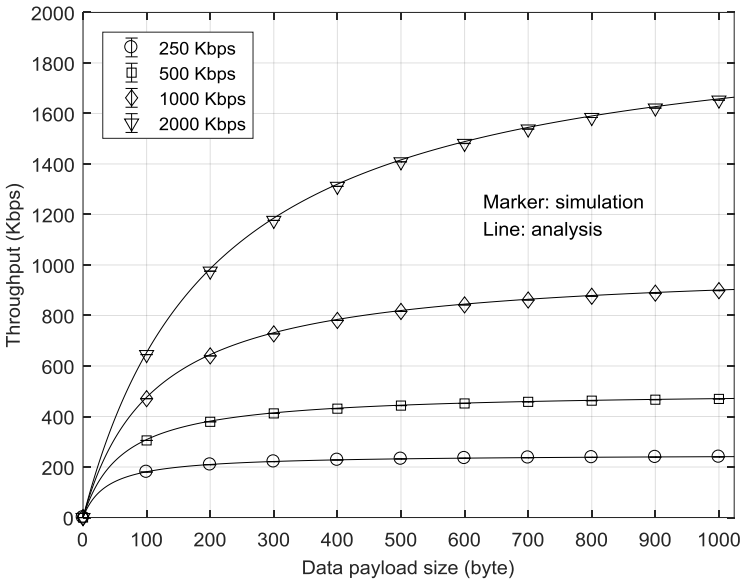

(a) When $\rho = 0$.

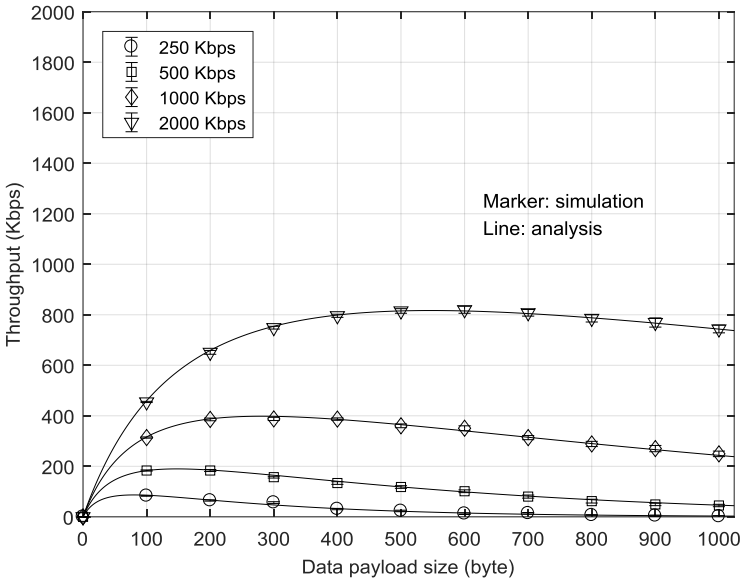

(b) When $\rho = 0.2$.

Fig. 4-3. Throughput according to the payload size.

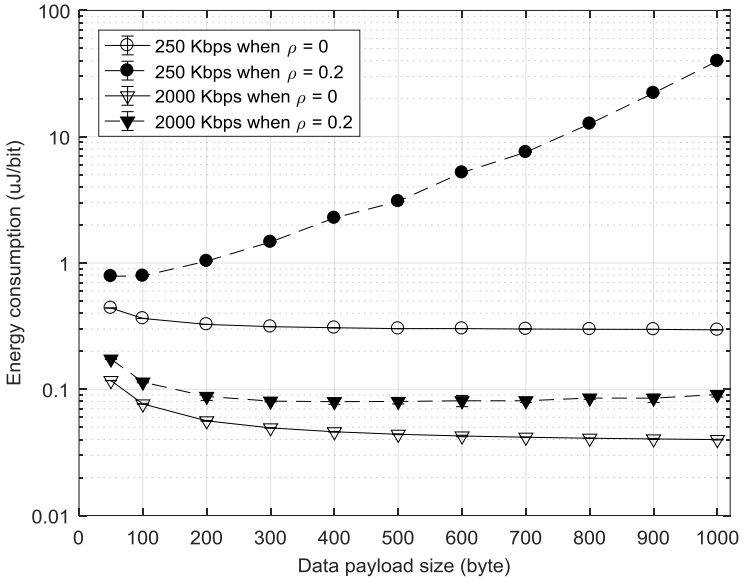

Fig. 4-4. Energy consumption according to the payload size.

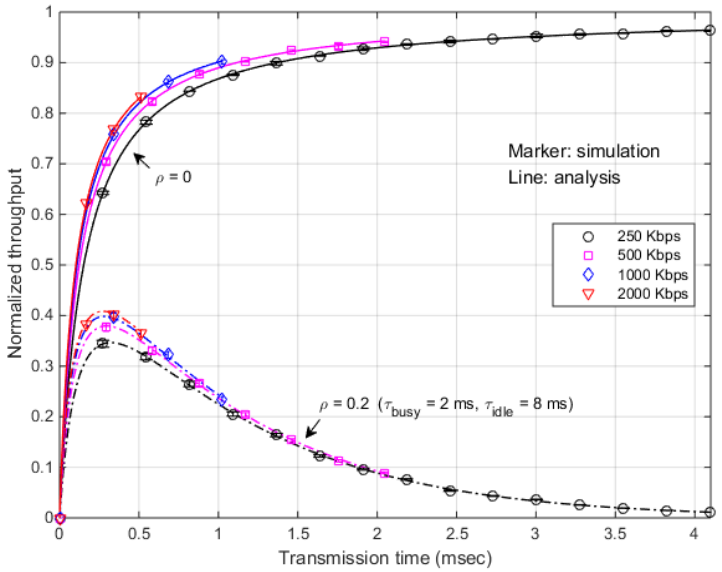

Fig. 4-5. Normalized throughput according to the transmission time.

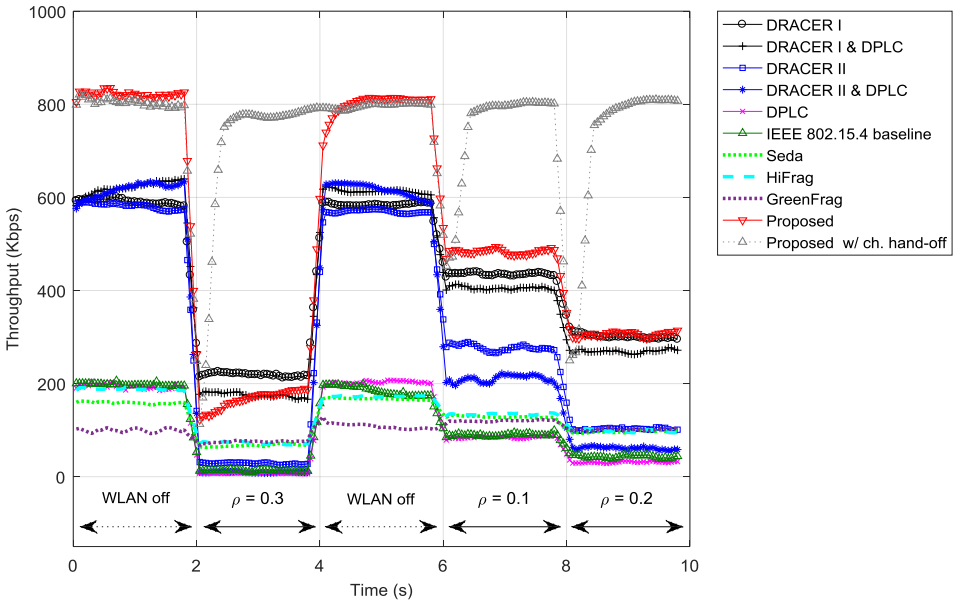

(a) When $L = 300$ bytes .

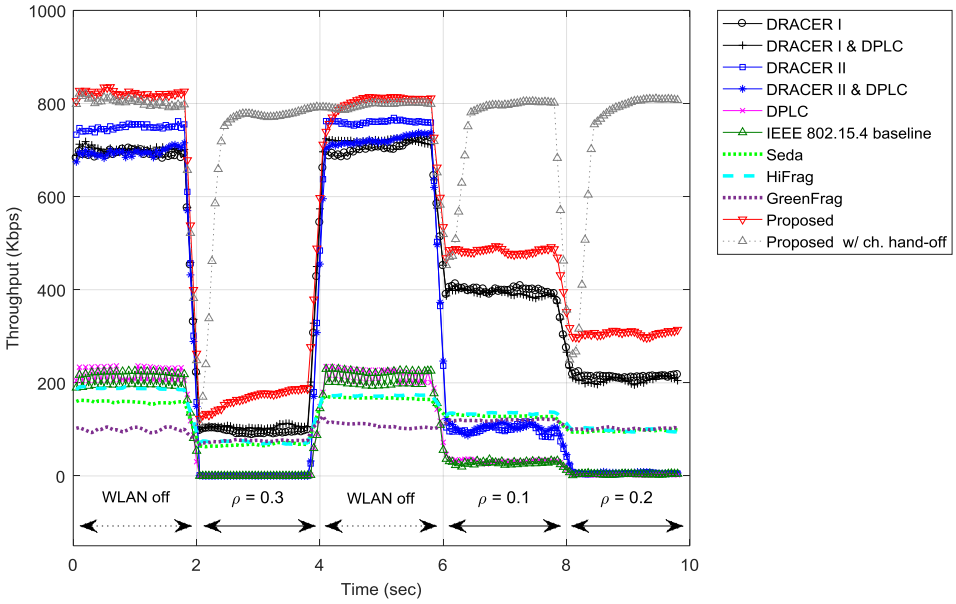

(b) When $L = 1000$ bytes .

Fig. 4-6. Throughput according to the change of interference.

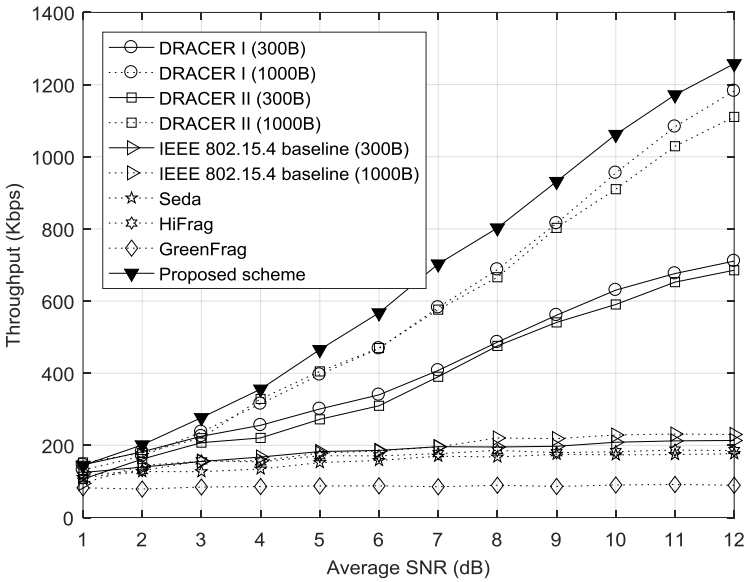

(a) When $\rho = 0$.

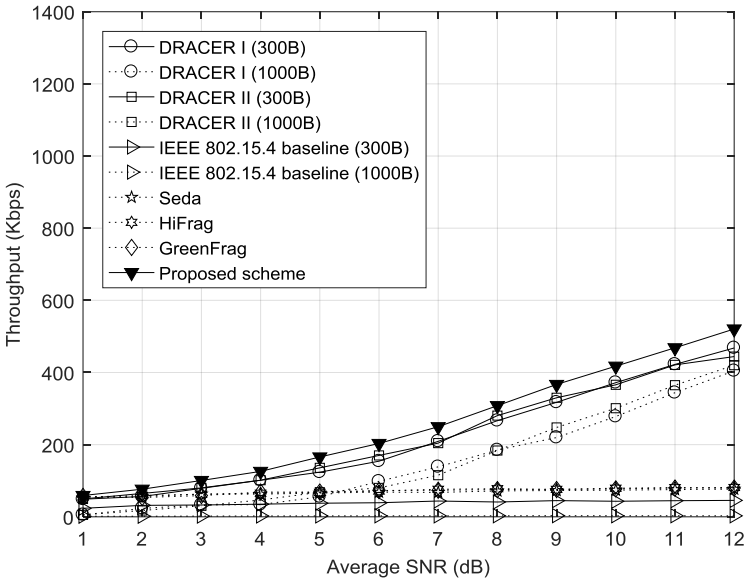

(b) When $\rho = 0.2$.

Fig. 4-7. Throughput according to the SNR.

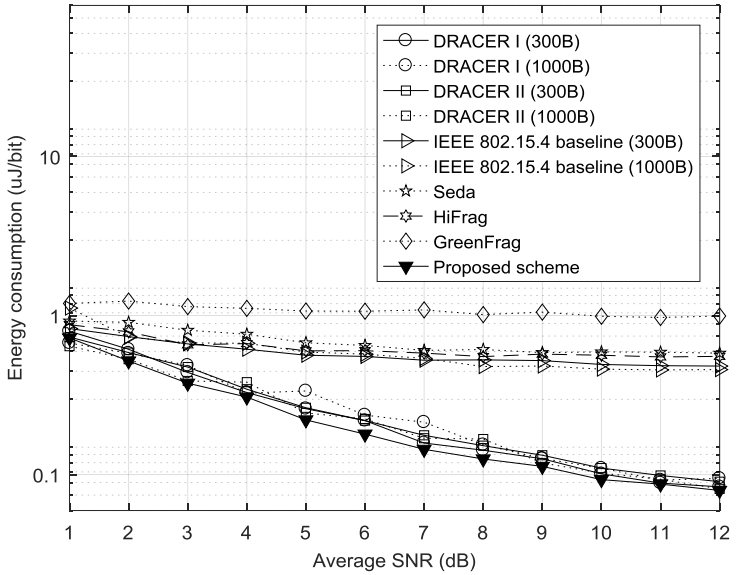

(a) When $\rho = 0$.

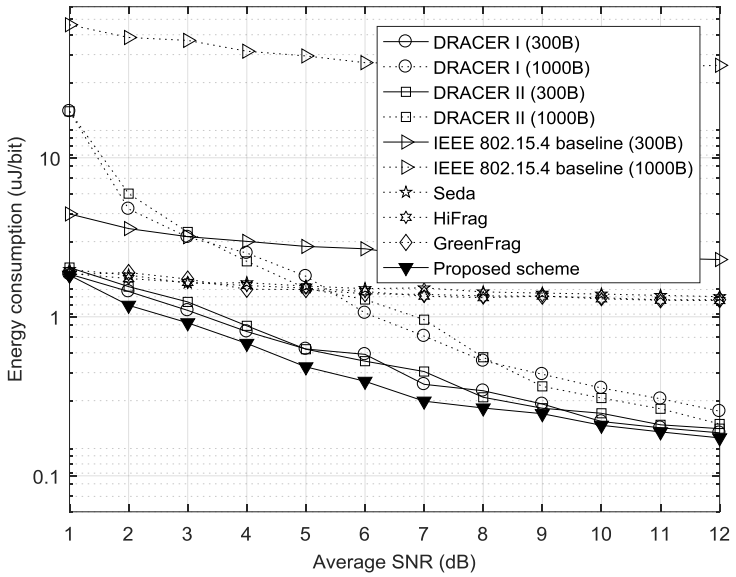

(b) When $\rho = 0.2$.

Fig. 4-8. Energy consumption according to the SNR.

Table 4-2. Transmission delay according to the SNR (unit: sec).

SNR	2 dB		6 dB		12 dB	
ρ	0	0.2	0	0.2	0	0.2
DRACERI (300B)	**5.9**	19.0	3.9	7.0	2.0	**3.0**
DRACERI (1000B)	6.9	46.0	2.9	11.0	**1.0**	**3.0**
DRACERII (300B)	6.9	17.0	3.9	7.0	2.0	**3.0**
DRACERII (1000B)	**5.9**	61.1	2.9	14.0	**1.0**	**3.0**
15.4 baseline (300B)	7.9	34.1	5.9	28.1	4.9	24.0
15.4 baseline (1000B)	7.9	690.4	5.9	396.8	4.9	396.8
Seda	8.8	19.0	6.9	16.0	5.9	14.0
HiFrag	8.8	18.0	6.9	15.0	5.9	14.0
GreenFrag	13.8	20.0	12.8	15.0	11.8	14.0
Proposed scheme	**5.9**	**14.0**	**2.0**	**6.0**	**1.0**	**3.0**

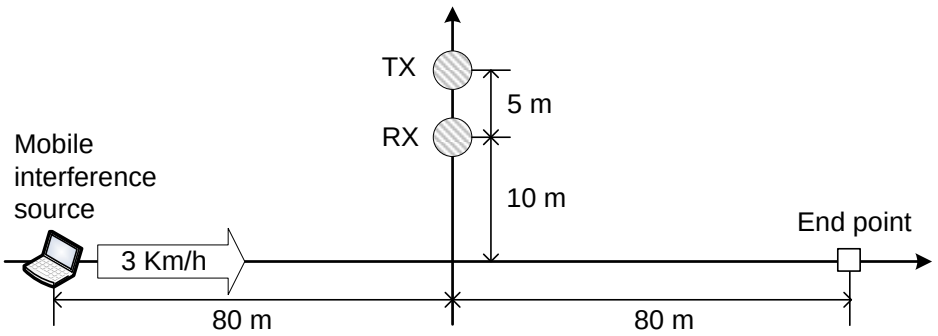

(a) Simulation scenario (without any shadowing).

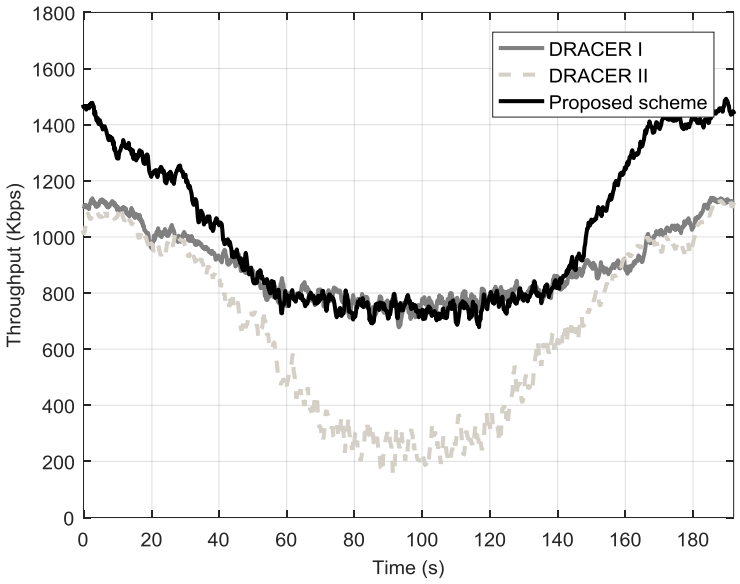

(b) Throughput according to time when the maximum R is 2 Mbps.

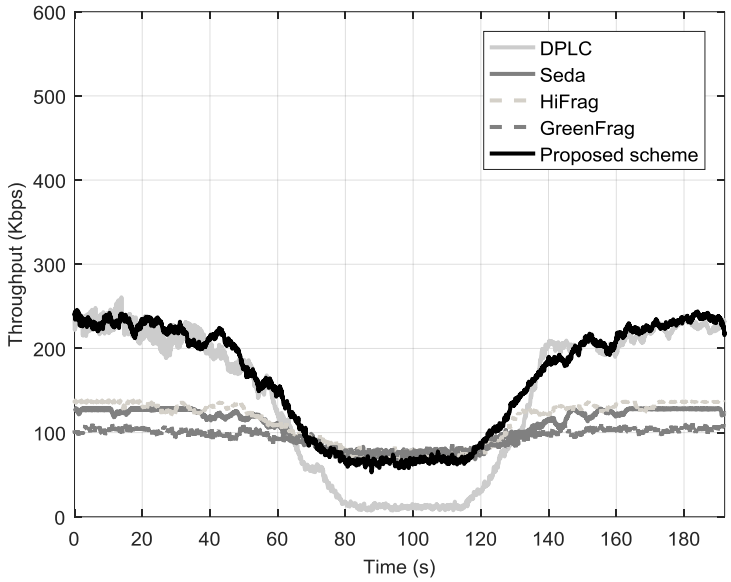

(c) Throughput according to time when the maximum R is limited to 250 Kbps.

Fig. 4-9. Transmission performance in the presence of mobile interference source.

Chapter 5

Conclusions

In this dissertation, we have considered the operation of low-power WSNs in the presence of co-channel interference. We have designed a low-power WSN transceiver that can provide stable performance in co-channel interference environments, while providing the backward compatibility with IEEE 802.15.4. The synchronized operation of a beacon-enabled cluster-tree WSN can stably be maintained in the presence of severe co-channel interference by repeatedly transmitting synchronization signal and making seamless channel hand-off in a channel-aware manner. The transmission performance can be improved by adjusting the transmission rate and the transmission time according to the change of operation environments. The analytic and simulation results show that the proposed scheme significantly improves throughput performance, while preserving energy efficiency even in the presence of severe interference. The design has been verified by computer simulation and experiments using motes in real environments. The design can be implemented with a marginal increase of complexity. The verification shows that the transceiver can provide performance quite robust to the co-channel

interference, making it applicable to commercial deployment of ZigBee-based low-power WSNs. We summarize some interesting future research directions below.

- **Self-healing**: WSN should be able to have fast self-healing capability without large signaling overhead. It has been shown that the proposed scheme can provide stable connectivity in the presence of severe co-channel interference. However, the proposed scheme may not work properly if connectivity is damaged due to some other causes such as interrupt of wireless link, depletion of battery and software or hardware failure. It is mainly because the proposed scheme makes child nodes first search for its parent node, yielding waste of time and energy in the case that the parent node may no more be reachable. It may be desirable to develop efficient self-healing scheme in consideration of the presence of co-channel interference and interference management scheme.
- **Transmission power**: Large-scale WSNs may seriously suffer from low traffic reliability mainly due to not only the presence of interference from coexisting radio systems but also signal collision among sensor nodes. Increasing transmission power may be effective for performance improvement in interference environments, but yield performance degradation due to increased collision inside the network[2]. Moreover, the transmission power may determine node density in the network, which directly affects the self-configuration of multi-hop network. It may be desirable to determine proper transmission power in consideration of network size and the maximum number of hops. It may also be desirable to develop network self-configuration scheme in consideration of transmission power, which can provide desired QoS even in harsh operation environments.

[2] The signal collision can be alleviated by decreasing transmission time. The proposed multi-rate transceiver can be used to reduce transmission time by employing higher transmission rate.

- **Low-power operation**: Energy saving is one of major concerns for low-power WSNs. If a node has considerably low data arrival rate, a better strategy in terms of energy saving may not be tracking the beacon frame. If a packet arrives at the node, the node will wake up and begin listening to the channel until it receives a beacon frame from its parent node. If the node finishes its data transaction, it may switch to a low-power sleep mode until next data arrival. If the proposed scheme is employed, synchronization time and power consumption of non-tracking nodes may increase. It is mainly because in the case that a parent node has changed its channel, its non-tracking child nodes may not know in which channel its parent node is operating when it wakes up. It may be required to design energy-efficient synchronization scheme for the non-tracking operation in consideration of data arrival rate, beacon interval, the number of candidate channels, etc.
- **Packet recovery**: The lack of interference-free channels has led researchers to work on so-called packet recovery. For example, BuzzBuzz studied the interplay between 802.11 and 802.15.4, and applied an FEC scheme against interference for ZigBee devices [29]. Some previous works focused on exploiting the temporal effects of interference such as variations in reception errors [65, 66] or received signal strength [67] to localize corrupted segments and retransmit only the corrupted segments. CrossZig may recognize interference patterns by analyzing physical layer hints (e.g., signal power, Hamming distance and demodulation soft values) and harness that to adapt the recovery mechanism [68]. It may be desirable to use and/or develop packet recovery scheme applicable for low-power and low-complexity devices to further improve the coexistence performance of low-power WSNs in unlicensed spectrum band.

Appendix

A. Average synchronization time during frequency hopping

We calculate the average synchronization time when a child device is synchronized with its cluster head through hopping channel i ($\in \Omega = \{1,2,\ldots,M\}$) in the frequency hopping mode. The average synchronization time T_{Ω} can be computed as

$$T_{\Omega} = \sum_{i=1}^{M} \pi_i T_{\Omega|i} \tag{A.1}$$

where π_i denotes the probability of synchronization on channel i and and $T_{\Omega|i}$ denotes the expected synchronization time after being synchronized on channel i. Then, it can be shown that

$$\begin{aligned} \pi_i &= \frac{1-p_i}{(1-p_1)+(1-p_2)+\cdots+(1-p_M)} \\ &= \frac{1-p_i}{M(1-p_{\Omega})}, \end{aligned} \tag{A.2}$$

$$T_{\Omega|i} = \frac{1+\tilde{p}_{i+1}+\tilde{p}_{i+1}\tilde{p}_{i+2}+\cdots+\tilde{p}_{i+1}\cdots\tilde{p}_{i+M-1}}{1-p_1p_2\cdots p_M} T_{BI}^1 \tag{A.3}$$

where $\tilde{p}_i = p_{\mathrm{mod}\{(i-1)/M\}+1}$. Finally, the average synchronization time T_Ω can be represented as

$$\begin{aligned} T_\Omega &= \sum_{i=1}^{M} \frac{1-p_i}{M(1-p_\Omega)} \cdot \frac{1+\tilde{p}_{i+1}+\tilde{p}_{i+1}\tilde{p}_{i+2}+\cdots+\tilde{p}_{i+1}\cdots\tilde{p}_{i+M-1}}{1-p_1p_2\cdots p_M} T_{BI}^1 \\ &= \frac{M(1-p_1p_2\cdots p_M)}{M(1-p_\Omega)(1-p_1p_2\cdots p_M)} T_{BI} \\ &= \frac{1}{1-p_\Omega} T_{BI}. \end{aligned} \tag{A.4}$$

It can be seen from (A.4) that T_Ω is inversely proportional to the probability of beacon reception on channels in Ω (i.e., $1-p_\Omega$) .

B. Derivation of (4.2)

It can be shown that the PER without channel coding in the presence of interference can be represented as

$$p = 1-\left(1-b(\gamma_{\mathrm{SNR}})\right)^{L_{\mathrm{pkt}}-L_{\mathrm{int}}}\left(1-b(\gamma_{\mathrm{SINR}})\right)^{L_{\mathrm{int}}} \tag{B.1}$$

where $b(\gamma)$ denotes the BER at an SNR of γ, γ_{SNR} denotes the SNR in the absence of interference, γ_{SINR} denotes the SINR in the presence of interference signal, L_{pkt} denotes the bit size of a packet, and L_{int} $\left(\le L_{\mathrm{pkt}}\right)$ denotes the number of bits collided with interference signal. Since L_{int} can randomly be changed, the average PER can be represented as

$$\begin{aligned}\bar{p} &= E_{L_{\text{int}}}[p] \\ &= 1-(1-p_s)E_{L_{\text{int}}}\left[K^{L_{\text{int}}}\right]\end{aligned} \tag{B.2}$$

where $p_s = 1-(1-b(\gamma_{\text{SNR}}))^{L_{\text{pkt}}}$ and $K = (1-b(\gamma_{\text{SINR}}))/(1-b(\gamma_{\text{SNR}}))$. Note that $0.5 < K < 1$ since $0 < b(\gamma_{\text{SNR}}) < 0.5$, $0 < b(\gamma_{\text{SINR}}) < 0.5$ and $b(\gamma_{\text{SNR}}) < b(\gamma_{\text{SINR}})$. Without information on the probability distribution function of L_{int}, it may not be easy to calculate the expectation. For ease of calculation, define a random variable φ by

$$\varphi = \begin{cases} 1 & ; L_{\text{int}} = \\ 0 & ; L_{\text{int}} > \end{cases} . \tag{B.3}$$

It can be shown from $\varphi \le K^{L_{\text{int}}}$ for all L_{int} that

$$\begin{aligned}\tilde{p} &= 1-(1-p_s)(1-p_c) \\ &\ge 1-(1-p_s)E_{L_{\text{int}}}\left[K^{L_{\text{int}}}\right] = \bar{p}\end{aligned} \tag{B.4}$$

where p_c denotes the probability of transmission failure assuming that the packet transmission is failed whenever the collision occurs, and equals to $1-E_{L_{\text{int}}}[\varphi]$. The assumption may be valid if SINR is sufficiently low. Table B-1 summarizes pairs of γ_{SINR} and L_{int} yielding $K^{L_{\text{int}}} < 0.01$ for IEEE 802.15.4 communications.

Table B-1. Conditions making $K^{L_{\text{int}}} < 0.01$ for IEEE 802.15.4 communications.

$b(\gamma_{\text{SINR}})$	0.01	0.1	0.2	0.3	0.4	0.44
γ_{SINR}	-2.5 dB	-5.6 dB	-7.5 dB	-9.5 dB	-12.5 dB	-14.6 dB
L_{int}	57.3 bytes	5.5 bytes	2.6 bytes	1.6 bytes	1.1 bytes	< 1 byte

References

[1] H.-S. Kim, H. Cho, M.-S. Lee, J. Paek, J.-G. Ko and S. Bahk, "MarketNet: An Asymmetric Transmission Power-based Wireless System for Managing e-Price Tags in Markets," in *Proc. ACM Int. Conf. on Embedded networked sensor systems (SenSys)*, pp. 281-294, Nov. 2015.

[2] IEEE Std. 802.15.4-2006: IEEE standard for wireless medium access control (MAC) and physical layer (PHY) specifications for low-rate wireless personal area networks (LR-WPANs), 2006.

[3] A. Wheeler, "Commercial Applications of Wireless Sensor Networks Using ZigBee," *IEEE Commun. Mag.*, vol. 45, no. 4, pp. 70-77, Apr. 2007.

[4] P. Huang, L. Xiao, S. Soltani, M.-W. Mutka, and N. Xi, "The Evolution of MAC Protocols in Wireless Sensor Networks: A Survey," *IEEE Commun. Surveys & Tutorials*, vol. 15, no. 1, pp. 101-120, First quarter 2013.

[5] Y.-K. Huang, A-C. Pang and H.-N. Hung, "A Comprehensive Analysis of Low-Power Operation for Beacon-enabled IEEE 802.15.4 Wireless Networks," *IEEE Trans. Wireless Commun.*, vol. 8, no. 11, pp. 5601-5611, Nov. 2009.

[6] "ZigBee Specification," *ZigBee Document 053474r17 Version*, pp. 1-576, 2008.

[7] H.-S. Kim, J.-S. Bang, and Y.-H. Lee, "Distributed Network Configuration in Large-scale Low Power Wireless Networks," *Computer Networks*, vol. 70, pp. 288-301, Sept. 2014.

[8] J.-S. Han, H.-S. Kim, J.-S. Bang and Y.-H. Lee, “Interference Mitigation in IEEE 802.15.4 Networks,” in *Proc. IEEE Global Commun. Conf. (Globecom)*, pp. 1-5, Dec. 2011.

[9] J.-S. Han, T.-H. Kim and Y.-H. Lee, “Robust Transmission of the IEEE 802.15.4 Signal in the Presence of Co-channel Interference,” in *Proc. IEEE Wireless Commun. and Networking Conf. (WCNC)*, pp. 53-58, Apr. 2013.

[10] A. Sikora and V. Groza, “Coexistence of IEEE 802.15.4 with Other Systems in the 2.4GHz-ISM-Band,” in *Proc. IEEE Instrumentation and Measurement Tech. Conf. (IMTC)*, pp. 1786-1791, May 2005.

[11] S.-Y. Shin, H.-S. Park, S. Choi and W.-H. Kwon, “Packet Error Rate Analysis of ZigBee under WLAN and Bluetooth Interferences,” *IEEE Trans. Wireless Commun.*, vol. 6, no. 8, pp. 2825-2830, Aug. 2007.

[12] L. Angrisani, M. Bertocco, D. Fortin and A. Sona, “Experimental Study of Coexistence Issues between IEEE 802.11b and IEEE 802.15.4 Wireless Networks,” *IEEE Trans. Instrumentation and Measurement*, vol. 57, no. 8, pp. 1514-1523, Aug. 2008.

[13] W. Yuan *et al.*, “Coexistence Performance of IEEE 802.15.4 Wireless Sensor Networks under IEEE 802.11b/g Interference,” *Wireless Personal Commun.* vol. 68, no. 2, pp. 281-302, Dec. 2011.

[14] W. Guo, W. M. Healy and M. Zhou, “Impacts of 2.4-GHz ISM band Interference on IEEE 802.15.4 Wireless Sensor Network Reliability in Buildings,” *IEEE Trans. Instrumentation and Measurement*, vol. 61, no. 9, pp. 2533-2544, Sept. 2012.

[15] D. Han and O. Gnawali, “Performance of RPL under Wireless Interference,” *IEEE Commun. Mag.*, vol. 51, no. 12, pp. 137-143, Dec. 2013.

[16] R. Musaloiu-E and A. Terzis, “Minimising the Effect of WiFi Interference in 802.15.4 Wireless Sensor Networks,” *Int. J. Sensor Networks*, vol. 3, no. 1, pp. 43-54, Jan. 2008.

[17] W. Xu, W. Trappe and Y. Zhang, “Defending Wireless Sensor Networks from Radio Interference through Channel Adaptation,” *ACM Trans. Sensor Networks*, vol. 4, no. 4, pp. 1-34, Aug. 2008.

[18] P. Yi, A. Iwayemi and C. Zhou, “Developing ZigBee Development Guideline under WiFi Interference for Smart Grid Applications,” *IEEE Trans. Smart Grid*, vol. 2, no. 1, pp. 110-120, Mar. 2011.

[19] L. Tytgat, O. Yaron, S. Pollin, In. Moerman, and P. Demeester, “Analysis and Experimental Verification of Frequency-Based Interference Avoidance Mechanisms in IEEE 802.15.4,” *IEEE/ACM Trans. Networking*, vol. 23, no. 2, pp. 369-382, Apr. 2015.

[20] M. Shar, G. Hackmann and C. Lu, “ARCH: Practical Channel Hopping for Reliable Home-area Sensor Networks,” in *Proc. IEEE Real-Time and Embedded Tech. and App. Symp. (RTAS)*, pp. 305-315, Apr. 2011.

[21] V. Iyer, M. Woehrle and K. Langendoen, “Chrysso – A Multi-channel Approach to Mitigate External Interference,” in *Proc. IEEE Conf. on Sensor, Mesh and Ad Hoc Commun. And Networks (SECON)*, pp. 449-457, June 2011.

[22] W. Jeong and J. Lee, “Performance Evaluation of IEEE 802.15.4e DSME MAC Protocol for Wireless Sensor Networks,” in *Proc. IEEE Workshop on Enabling Technologies for Smartphone and Internet of Things (ETSIoT)*, pp. 7–12, 2012.

[23] C. Gomez, J. Oller and J. Paradells, "Overview and Evaluation of Bluetooth Low Energy: An Emerging Low-Power Wireless Technology," *Sensors*, vol. 12, no. 9, pp. 11734-11753, Aug. 2012.

[24] J. Huang, G. Xing, G. Zhou and R. Zhou, "Beyond Co-existence: Exploiting WiFi White Space for ZigBee Performance Assurance," in *Proc. IEEE Int. Conf. on Network Protocols (ICNP)*, pp. 305-314, Oct. 2010.

[25] S.-H. Lee, H.-S. Kim, and Y.-H. Lee, "Mitigation of Co-channel Interference in Bluetooth Piconets," *IEEE Trans. Wireless Commun.*, vol. 11, no. 4, pp. 1249-1254, Apr. 2012.

[26] M. Sha, G. Hackmann and C. Lu, "Real-world Empirical Studies on Multi-channel Reliability and Spectrum Usage for Home-area Sensor Networks," *IEEE Trans. Network and Service Management*, vol. 10, no. 1, pp. 56-69, Mar. 2013.

[27] X. Zhang and K.-G. Shin, "Cooperative Carrier Signaling: Harmonizing Coexisting WPAN and WLAN Devices," *IEEE/ACM Trans. Networking*, vol. 21, no. 2, pp. 426-439, Apr. 2013.

[28] J. Hou, B. Chang, D.-K. Cho and M. Gerla, "Minimizing 802.11 Interference on ZigBee Medical Sensors," in *Proc. ACM Int. Conf. on Body Area Networks (BodyNets)*, pp. 1-8, Apr. 2009.

[29] C.-J. M. Liang, N. B. Priyantha, J. Liu and A. Terzis, "Surviving Wi-Fi Interference in Low Power ZigBee Networks," in *Proc. ACM Int. Conf. on Embedded networked sensor systems (SenSys)*, pp. 309-322, Nov. 2010.

[30] P. Guo, J. Cao, K. Zhang and X. Liu, "Enhancing ZigBee Throughput under WiFi Interference Using Real-time Adaptive Coding," in *Proc. IEEE Conf. on Computer Commun. (INFOCOM)*, pp. 2858-2866, Apr. 2014.

[31] S. Lanzisera, A. M. Mehta and K. Pister, “Reducing Average Power in Wireless Sensor Networks through Data Rate Adaptation,” in *Proc. IEEE Int. Conf. on Commun. (ICC),* pp. 1-6, June 2009.

[32] W. Dong *et al*., “Dynamic Packet Length Control in Wireless Sensor Networks,” *IEEE Trans. Wireless Commun.*, vol. 13, no. 3, pp. 1172-1181, Mar. 2014.

[33] S. Chouldhury and J.-D. Gibson, “Payload Length and Rate Adaptation for Multimedia Communications in Wireless LANs,” *IEEE J. Sel. Areas in Commun.*, vol. 25, no. 4, pp. 796-807, May 2007.

[34] R. K. Ganti, P. Jayachandra, H. Luo and T. F. Abdelzaher, “Datalink Streaming in Wireless Sensor Networks,” in *Proc. ACM Int. Conf. on Embedded networked sensor systems (SenSys),* pp. 209-222, Nov. 2006.

[35] A. Shaowail *et el*., “iFrag: Interference-Aware Frame Fragmentation Scheme for Wireless Sensor Networks,” *ACM J. Wireless Networks,* vol. 20, no. 4, pp. 2019-2036, May 2014.

[36] A. Meer, A. Daghistani and B. Shihada, “An Energy Efficient Hybrid Interference-resilient Frame Fragmentation for Wireless Sensor Networks,” in *Proc. IEEE Int. Symp. on Personal, Indoor and Mobile Radio Commun. (PIMRC),* pp. 1024-1029, Aug. 2015.

[37] A. Daghistani, A. B. Khalifa, A. Showail and B. Shihada, “Green Partial Packet Recovery in Wireless Sensor Networks,” *J. Network and Computer Applications,* vol. 58, pp. 267-279, Dec. 2015.

[38] X. Zhang and K.-G. Shin, “E-MiLi: Energy-Minimizing Idle Listening in Wireless Networks,” *IEEE Trans. Mobile Computing*, vol. 11, no. 9, pp. 1441-1454, Sept. 2012.

[39] J. Suhonen, T.-D Hamalainen, and M. Hannikainen, “Availability and End-to-end Reliability in Low Duty Cycle Multihop Wireless Sensor Networks,” *Sensors*, vol. 9, pp. 2088-2116, 2009.

[40] C. Won, J. H. Youn, H. A. Sharif, and J. Deogun, “Adaptive Radio Channel Allocation for Supporting Coexistence of 802.15.4 and 802.11b,” in *Proc. IEEE Veh. Tech. Conf. (VTC) Fall*, vol. 4, pp. 2522-2526, Sept. 2005.

[41] M.S. Kang, J.W. Chong, H. Hyun and D.K. Sung, “Adaptive Interference-aware Multi-channel Clustering Algorithm in a ZigBee Network in the Presence of WLAN Interference,” in *Proc. Int. Symp. on Wireless Pervasive Computing (ISWPC)*, pp. 200-205, Feb. 2007.

[42] IEEE Std. 802.15.4e-2012, Part 15.4: low-rate wireless personal area networks (LR-WPANs) amendment 1: MAC sub-layer, Apr. 2012.

[43] S. Geirhofer, L. Tong and B.-M Sadler, “Cognitive Medium Access: Constraining Interference Based on Experimental Models,” *IEEE J. Sel. Areas in Commun.*, vol. 26, no.1, pp. 95-105, Jan. 2008.

[44] I. Glaropoulos, A.-V. Luna, V. Fodor, and M. Papadopouli, “Closing the Gap between Traffic Workload and Channel Occupancy Models for 802.11 Networks,” *Ad Hoc Networks*, vol. 21, pp. 60-83, May 2014.

[45] TELOSB Mote Platform, Available: http://www.willow.co.uk/html/telosb_mote_platform.html, May 2012.

[46] G. Werner-Allen, K. Lorincz, M. Welsh, O. Marcillo, J. Johnson, M. Ruiz, and J. Lees, “Deploying a Wireless Sensor Network on an Active Volcano,” *IEEE Internet Computing*, vol. 10, no. 2, pp. 18-25, Mar. 2006.

[47] K. Chebrolu, B. Raman, N. Mishra, P. K. Valiveti, and R. Kumar, "BriMon: A Sensor Network System for Railway Bridge Monitoring," in *Proc. ACM Int. Conf. on Mobile systems, applications and services (MobiSys)*, pp. 2-14, June 2008.

[48] J. Paek, K. Chintalapudi, J. Cafferey, R. Govindan, and S. Masri, "A Wireless Sensor Network for Structural Health Monitoring: Performance and Experience," in *Proc. IEEE Workshop on Embedded Networked Sensors (EmNetS-II)*, May 2005.

[49] S. Kim, S. Pakzad, D. Culler, J. Demmel, G. Fenves, S. Glaser, and M. Turon, "Health Monitoring of Civil Infrastructures Using Wireless Sensor Networks," in *Proc. IEEE Int. Symp. on Information Processing in Sensor Networks (IPSN)*, pp. 254-263, Apr. 2007.

[50] L. Bello and E. Toscano, "Coexistence Issues of Multiple Co-located IEEE 802.15.4/ZigBee Networks Running on Adjacent Radio Channels in Industrial Environments," *IEEE Trans. Industrial Informatics*, vol. 5, no. 2, pp. 157-167, May 2009.

[51] Y.-C. Liang *et al*., "Sensing-throughput Tradeoff for Cognitive Radio Networks," *IEEE Trans. Wireless Commun.*, vol. 7, no. 4, pp. 1326-1337, Apr. 2008.

[52] M. Park, "Specification framework for TGah," *IEEE 802.11-11/1137r14*, Mar. 2013.

[53] "LoRaWAN™ Specification," *LoRa Alliance*, pp. 1-82, Jan. 2015.

[54] Farproc, "Wifi Analyzer," Google Play Store, Vers. 3.9.3, http://wifianalyzer.mobi, 2015.

[55] Texas Instruments, CC2420 Datasheet, Available: http://focus.ti.com/lit/ds/symlink/cc2420.pdf, 2010.

[56] J.-H. Hauer, "TKN15.4: An IEEE 802.15.4 MAC implementation for TinyOS 2," Telecommunication Networks Group, Technical Univ. Berlin, Tech. Rep. TKN-08-003, Mar. 2009.

[57] D-ITG distributed internet traffic generator, http://www.grid.unina.it/software/ITG/.

[58] R.-J. Punnoose *et al*., "Efficient Simulation of Ricean Fading within a Packet Simulator," in *Proc. IEEE Veh. Tech. Conf. (VTC)*, pp. 764-767, Sept. 2000.

[59] I. Ramachandran and S. Roy, "On the Impact of Clear Channel Assessment on MAC Performance," in *Proc. IEEE Global Commun. Conf. (Globecom)*, pp. 1-5, Nov. 2006.

[60] IEEE Std. 802.15.4g-2012, Part 15.4: Low Rate Wireless Personal Area Networks (LR-WPANs) Amendment 3: PHY Specifications for Low-Data-Rate, Wireless, Smart Metering Utility Networks, *IEEE*, Apr. 2012.

[61] X. Jin, Q. Zhang, P. Zeng, F. Kong, Y. Xiao, "Collision-free Multichannel Superframe Scheduling for IEEE 802.15.4 Cluster-tree Networks," *Int. J. Sensor Networks*, vol. 15, no. 4, pp. 246-258, Aug. 2014.

[62] W. Lee, K. Hwang, Y. Jeon and S. Choi, "Distributed Fast Beacon Scheduling for Mesh Networks," in *Proc. IEEE Int. Conf. on Mobile Adhoc and Sensor Systems (MASS)*, pp. 727-732, Oct. 2011.

[63] Atmel, AT86RF231 Datasheet, 2009.

[64] F. Qin and J. E. Mitchell, "Performance Estimation of Adaptive Spreading Code Length for Energy Efficient WSN," in *Proc. Wireless Advanced (WiAd)*, pp. 81-84, June 2011.

[65] G. Woo, P. Kheradpour, D. Shen and D. Katabi, “Beyond the Bits: Cooperative Packet Recovery Using Physical Layer Information,” in *Proc. ACM Int. Conf. on Mobile Computing and Networking (MobiCom)*, pp. 147-158, Sept. 2007.

[66] K. Jamieson and H. Balakrishnan, “PPR: Partial Packet Recovery for Wireless Networks,” in *Proc. ACM Conf. on Applications, technologies, architectures, and protocols for computer communications (SIGCOMM)*, vol. 37, no. 4, pp. 409-420, Aug. 2007.

[67] J. Hauer, A. Willig and A. Wolisz, “Mitigating the Effects of RF Interference through RSSI-based Error Recovery,” in *Proc. European Conf. on Wireless Sensor Networks (EWSN)*, pp. 224-239, Feb. 2010.

[68] A. Hithnawi, S. Li, H. Shafagh, J. Gross and S. Duquennoy, “CrossZig: Combating Cross-technology Interference in Low-power Wireless Networks,” in *Proc. IEEE/ACM Int. Symp. on Information Processing in Sensor Networks (IPSN)*, Apr. *2016.*

Korean Abstract

대규모 무선 센서 네트워크에 대한 상용화 요구가 급증하고 있다. 그러나 지그비와 같은 기존의 저전력 무선 센서 네트워킹 기술들은 제한된 네트워크 확장성(50 개 이상 규모의 네트워크의 자율 구축이 어려움), 동일 채널 간섭에 대한 취약성, 큰 신호 부담 등을 포함한 기술적 한계들로 인해 대규모 무선 센서 네트워크 구축에 사용되지 못하고 있는 실정이다. 특히 저전력 무선 센서 네트워크는 IEEE 802.11 무선 지역 영역 네트워크(이하 무선랜) 같은 2.4 GHz 비면허 대역에서 공존하는 무선 통신 시스템으로부터 매우 큰 영향을 받는다. 비면허 대역의 간섭 문제는 대규모 저전력 무선 센서 네트워크의 상용 활성화를 방해하는 대표적인 원인 중 하나이다. 저전력 무선 센서 네트워크와 무선랜 간의 공존에 대한 연구가 오랫동안 진행되어 왔음에도 불구하고, 실제 운용 환경에서 네트워킹을 안정적으로 유지하고 신호 전송을 효율적으로 할 수 있는, 간섭에 강인한 저전력 무선 센서 네트워킹 기술은 아직 등장하지 않았다.

본 논문에서는 동일 채널 간섭이 존재하는 환경에서 저전력 무선 센서 네트워크의 성능 개선 방안을 고려한다. 이를 위해 먼저 무선랜 등 동일 채널 간섭이 존재하는 환경 하에서 저전력 무선 센서 네트워크 신호를 전송할 때 발생하는 간섭의 영향을 분석한다. 수학적 분석 결과를 바탕으로, 동일 채널 내에 존재하는 간섭에 강인하며, 동시에 IEEE 802.15.4 와 하위 호환성을 제공하는 저전력 무선 센서 네트워크 송수신기의 개선 방안을 제안한다.

본 논문은 동일 채널 간섭이 존재하는 환경에서 네트워크 연결성의 개선 방안을 제안한다. 제안 기법은 채널 인지 기반의 동기 신호 전송 기법과 채널 핸드오프(hand-off) 기법을 이용하여 저전력 무선 센서 네트워크의 연결성을 개선할 수 있다. 제안 기법은 채널 상태와 신호 부담을 고려하여 네트워크 동기를 신뢰성 있게 유지할 수 있도록 비컨 신호를 반복적으로 전송한다. 간섭 신호가 채널을 많이 점유한 경우에는, 클러스터 내의 모든 기기들이 임시적으로 채널 도약(hopping)을 수행하며 그 도약 채널들 중 가장 채널 상태가 좋은 채널로 끊김없이 채널 핸드오프를 수행한다. 컴퓨터를 이용한 모의실험 및 TelosB 모트를 이용한 실험을 통해 제안 기법은 무선랜 등 동일 채널 간섭이 존재하는 환경에서도 네트워크 연결성을 안정적으로 제공할 수 있음을 보인다.

본 논문은 동일 채널 간섭이 존재하는 환경에서 신호 전송 성능의 개선 방안을 제안한다. 제안 기법은 간섭 환경의 변화에 따라 전송 속도와 페이로드 크기를 적응함으로써 저전력 무선 센서 네트워크의 쓰루풋을 개선할 수 있다. 제안 기법은 간섭 환경에서의 전송 실패 확률 및 데이터 쓰루풋에 대한 수학적 분석을 이용하여 쓰루풋을 극대화할 수 있는 페이로드 크기를 결정할 수 있다. 본 논문에서는 정규화된(normalized) 쓰루풋을 극대화하는 전송 시간(transmission time)이 전송 속도(transmission rate)에 거의 영향을 받지 않으며, 간섭 상태에 영향을 받음을 보인다. 제안 기법은 상기 분석 결과를 이용하여 채널 상태와 간섭 상태가 변화함에 따라 전송 속도와 전송 시간을 개별적으로 제어한다. 모의실험을 통해 제안 기법은 기존 기법들과 비교해 동일 채널 간섭이 존재하는 환경에서 쓰루풋 성능을 크게 향상시키고 에너지 효율을 유지함을 보인다.

주요어: 저전력 무선 센서 네트워킹, 동일 채널 간섭, 간섭에 강인한 네트워킹, 가변 송수신기 구조, 지그비.

학번: 2012-30237